# Perceptually Motivated BRDF Comparison using Single Image SUPPLEMENTAL MATERIAL

V. Havran[1] J. Filip[2] K. Myszkowski[3]
[1]Faculty of Electrical Engineering, Czech Technical University in Prague, Czech Republic
[2]Institute of Information Theory and Automation of the CAS, Czech Republic
[3]MPI Informatik, Saarbrücken, Germany

A supplementary material to the paper *Perceptually Motivated BRDF Comparison using Single Image* submitted on 12th March 2016 to EGSR 2016 conference, paper1001.

It comprises:

1. Extension to Spatial and Angular Variability
2. Tested Materials and Optimized Surfaces
3. Histogram Coverage
4. Psychophysical Experiments Results
5. Results of Computational Metrics
6. Comparing Psychophysics vs. Objective Metrics
7. Correlation of Psychophysical Data vs. Objective Metrics
8. Application example: analytical BRDF models performance evaluation under point-light and environment illumination

Supplementary electronic material for this paper submission contains:
1. Movie of BTF comparison,
2. Source code of a C++ application for BRDF comparison on optimized surfaces,
3. Zipped TXT files listing incoming and outgoing directions for each pixel of optimized surfaces 2 and 3.

# 1 Extension to Spatial and Angular Variability

Finally, we tested our optimized surfaces for comparison of spatially-varying material appearance represented by BTFs (http://cg.cs.uni-bonn.de/en/projects/btfdbb/download/ubo2003/). We mapped each BTF onto the optimized surfaces by using Cartesian UV mapping. To extend the method from BRDF to BTF it is appropriate to render many images so that we move the BTF tile over the surface, for example in zigzag order, where one movement corresponded to the distance between two texels from the BTF dataset. In order to introduce the same amount of data to the image as for the BRDF compared to the whole dataset, it would be necessary to render all $256 \times 256$ images for each unique BTF shift. However, since the BTF is highly compressible, we used repeatable BTF tiles only of size $25 \times 25$ texels. Finally, we rendered only images for 200 shifts that we assume to be sufficient to represent the characteristics of repeatable BTF tiles used in the experiments.

To get the degraded model we used a BTF model based on linear factorization of all BTF images using PCA [KMBK03]. Finally, we computed average C-SSIM scores [LPU*13] across all pixels in the rendered pairs of images to obtain a single difference value between a reference BTF and degraded BTF data. We compared the difference between model results for 60 and 20 eigen-components. Fig. 1 shows an example of performance degradation in the BTF difference detection for different surfaces (refer also to the supplemental materials for a movie that illustrates this issue).

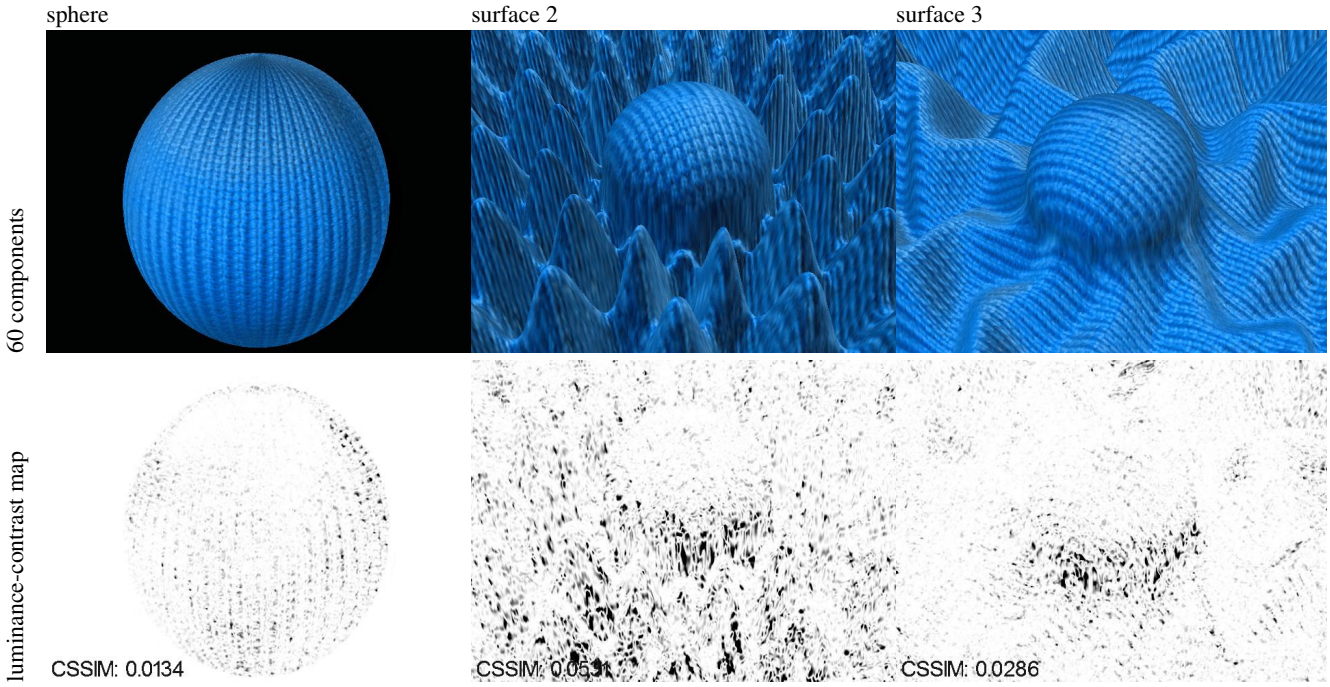


**Figure 1:** *Examples of BTF rendered on the sphere and optimized* surfaces 2 *and* 3*, together with C-SSIM luminance-contrast maps depicting differences due to using 20 PCA components instead of 60 (material knitted wool). Material wool, sphere: CSSIM = 0.0134, surface 2: CSSIM=0.0531, surface 3: CSSIM= 0.0286.*

Averaged values for over 200 of such shifts for three materials are shown in Fig 2. This graph reveals a significantly higher sensitivity of the optimized surfaces compared to the baseline sphere. *Surface 2*, whose sensitivity is higher by a factor of three, was found to be the best while the sensitivity of *surface 3* is double the baseline. The error-bars representing standard deviation across the tested 200 pixel shifts illustrate that C-SSIM differences for different shifts are negligible.

These results suggest that the optimized surfaces are appropriate also for more effective single-image comparisons of spatially-varying materials.

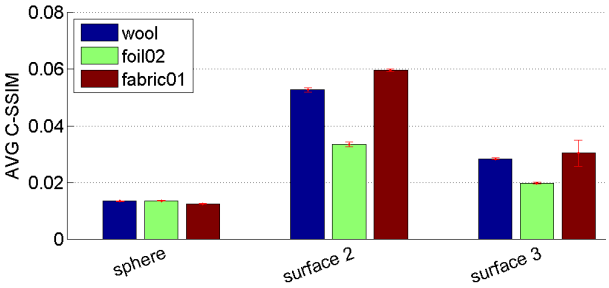


wool

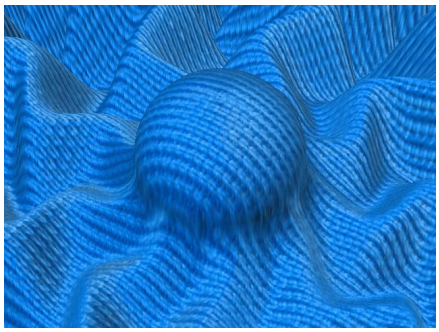

foil02

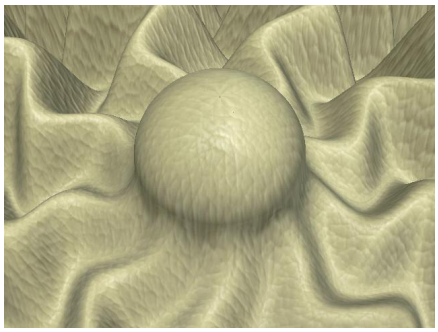

fabric01

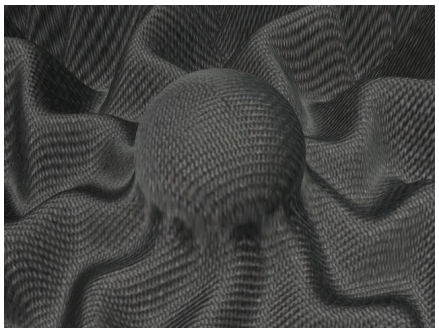

**Figure 2:** *Averaged C-SSIM values for surfaces* sphere, surface 2, *and* surface 3 *across three tested BTFs (shown below).*

### 1.1 Comparing BTFs

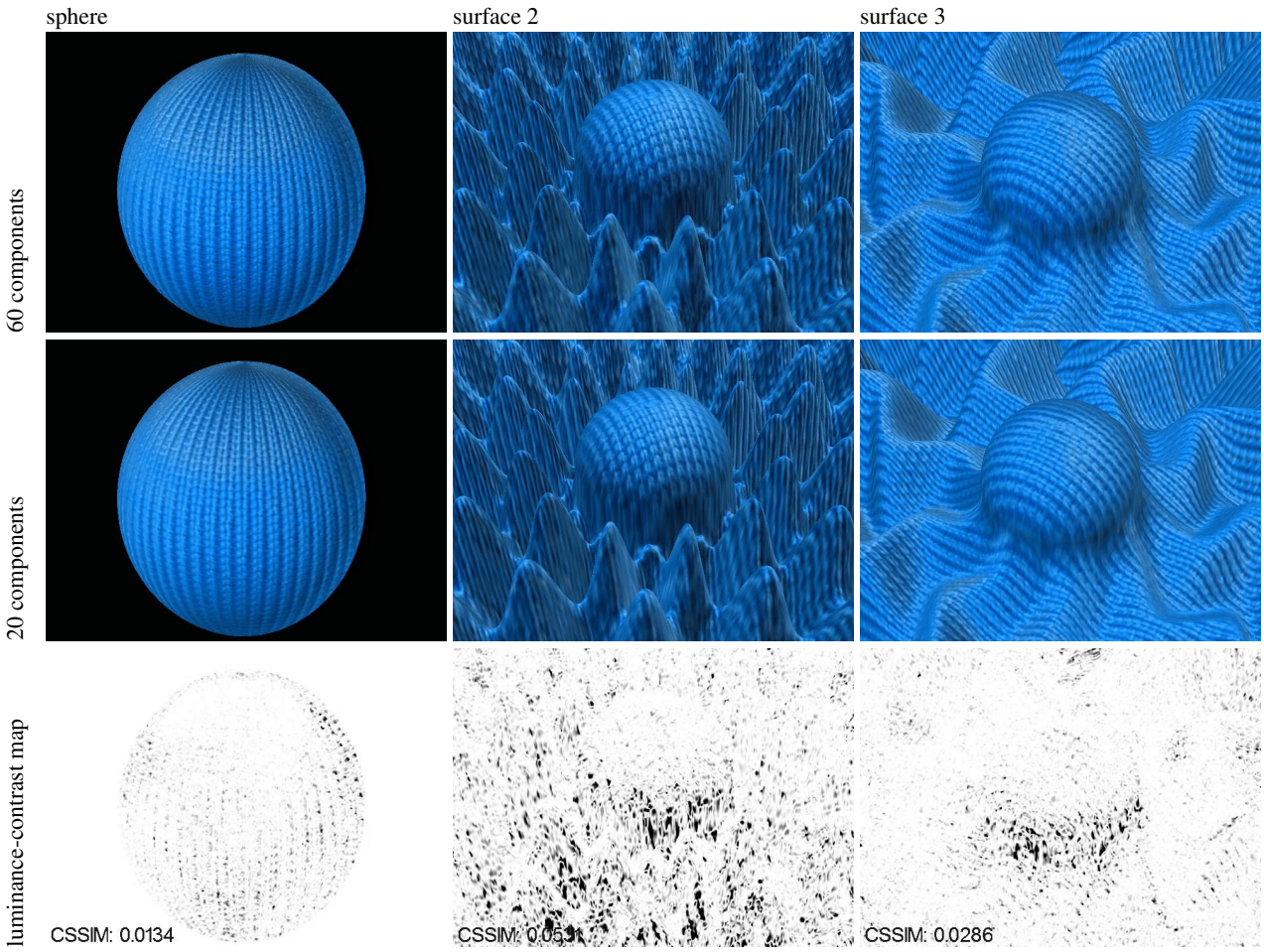


**Figure 3:** *Examples of BTF rendered on the sphere and optimized surfaces 2 and 3, together with CSSIM luminance-contrast maps depicting differences due to using 20 PCA components instead of 60 (material knitted wool).*

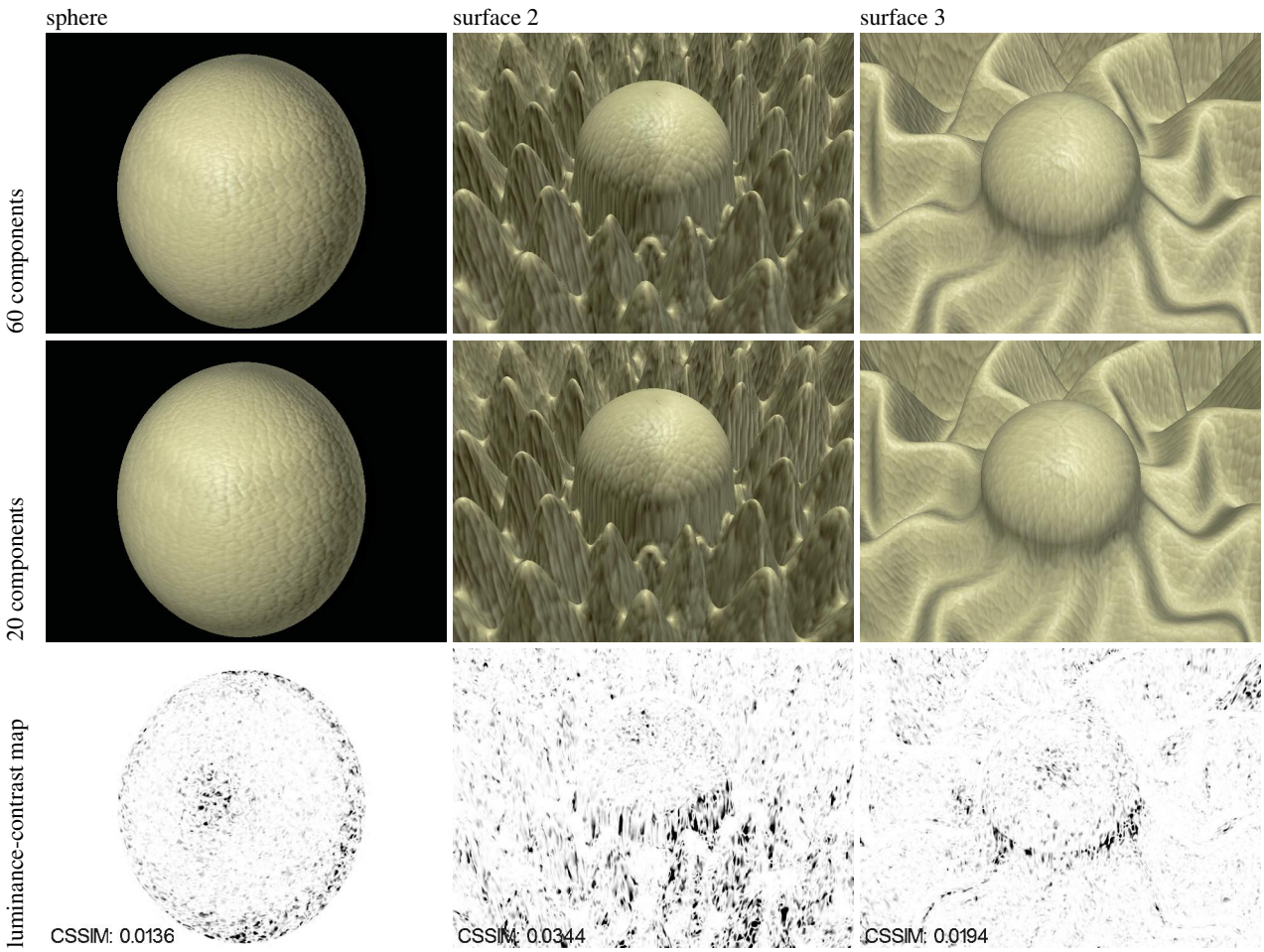


**Figure 4:** *Examples of BTF rendered on the sphere and optimized surfaces 2 and 3, together with CSSIM luminance-contrast maps depicting differences due to using 20 PCA components instead of 60 (material artificial leather).*

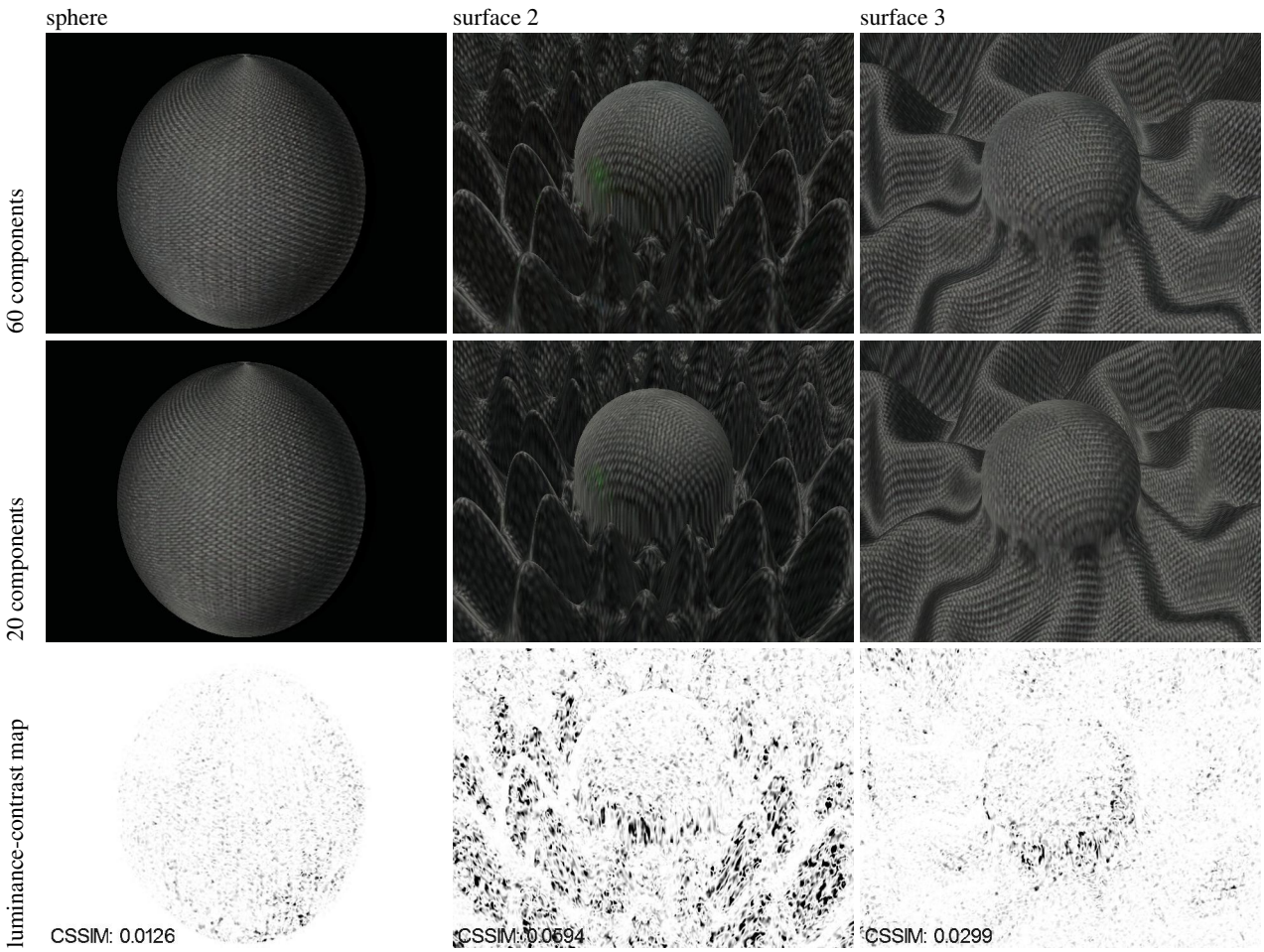


**Figure 5:** *Examples of BTF rendered on the sphere and optimized surfaces 2 and 3, together with CSSIM luminance-contrast maps depicting differences due to using 20 PCA components instead of 60 (material dark fabric).*

## 2 Tested Materials and Optimized Surfaces

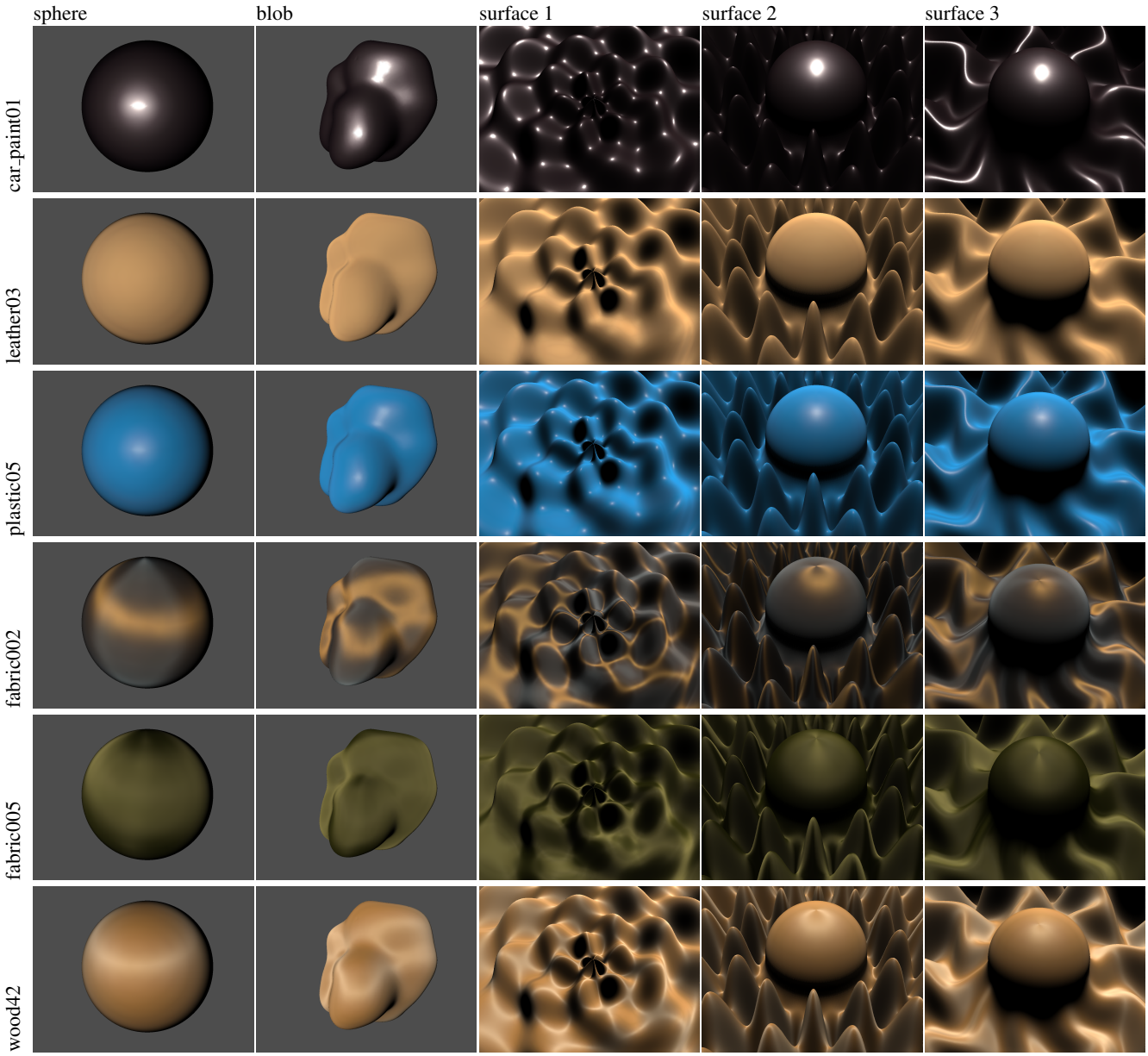


**Figure 6:** *The six tested materials (rows), first three isotropic ones, second three anisotropic ones on all tested surfaces (columns).*

## 3 Histogram Coverage

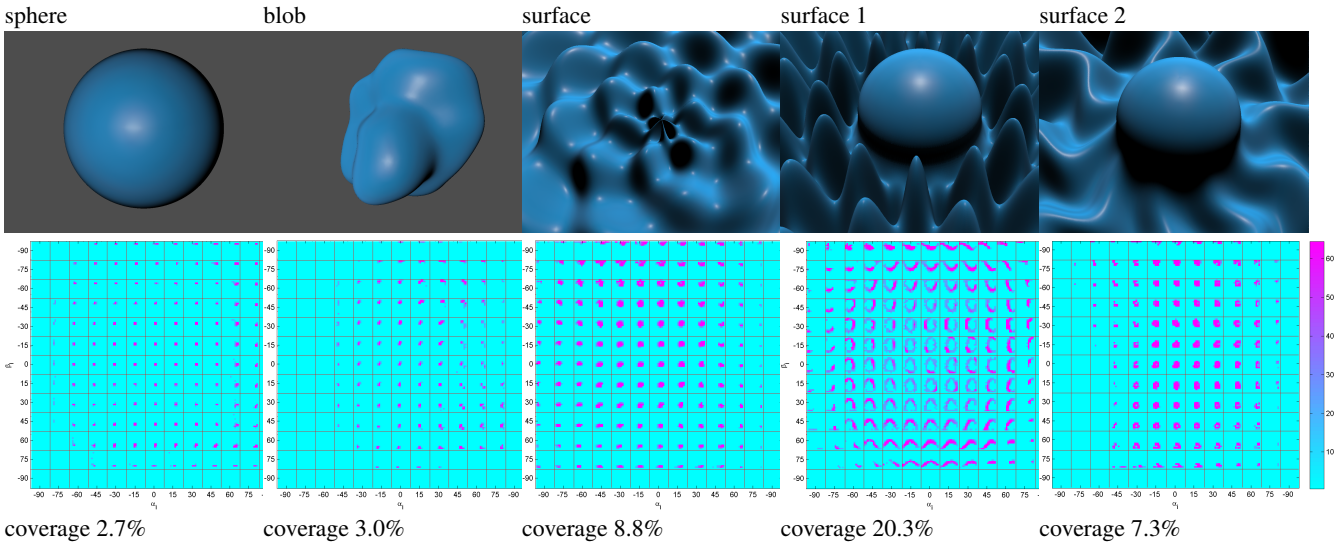


**Figure 7:** *Comparison of histograms of different tested surfaces: sphere, blob, and optimized surfaces 1, 2, and 3. Histogram are reshaped into 2D images showing coverage of the bins in onion-sliced parameterization by magenta values. Each small square block features histogram values dependent in* $\beta_i/\beta_v$.

## 4 Psychophysical Experiments Results

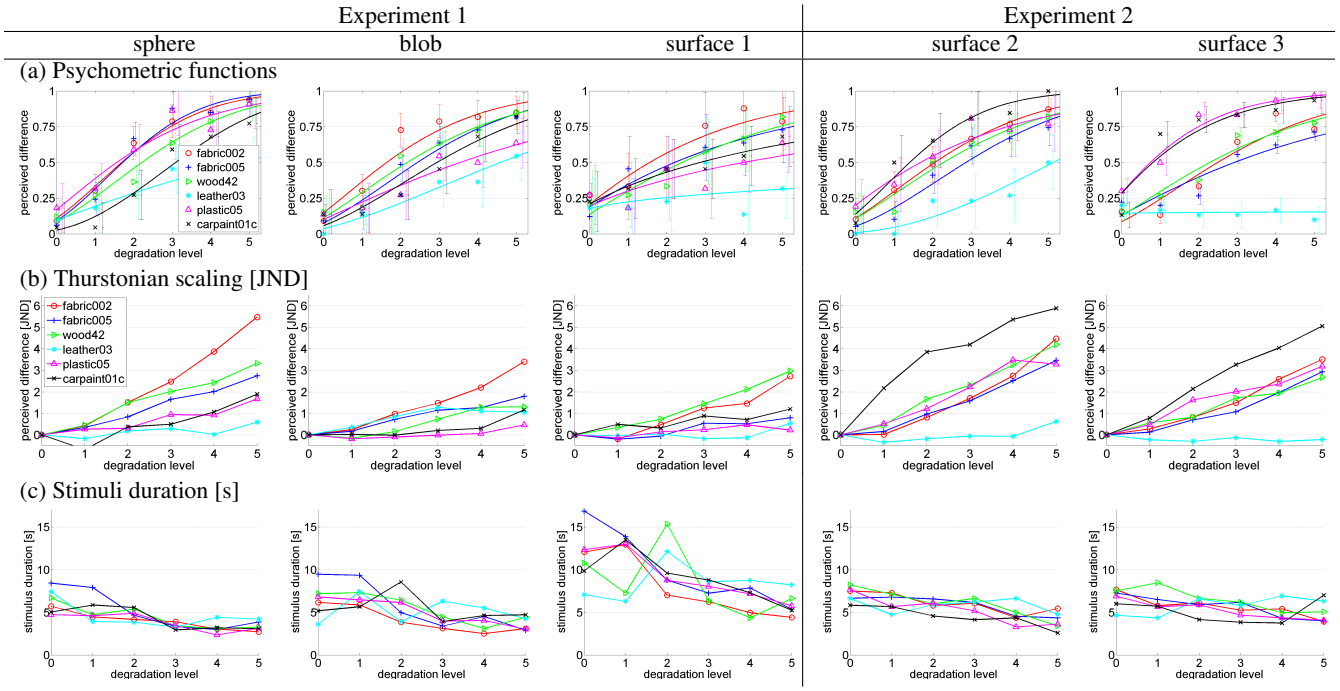


**Figure 8:** *Results of (a) psychometric fitting, (b) Thurstonian scaling, (c) stimuli duration.*

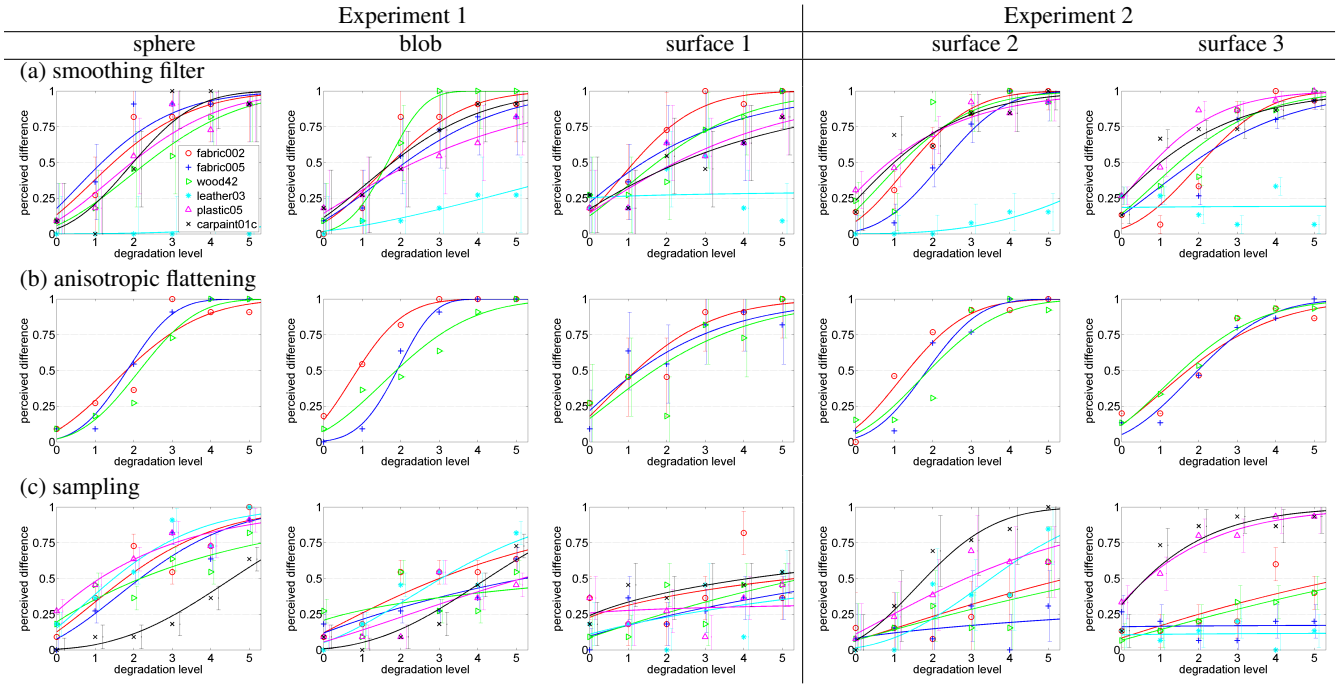


**Figure 9:** *Psychometric functions for different BRDF degradation filters (a) smoothing filter, (b) anisotropic flattening, (c) azimuthal resampling.*

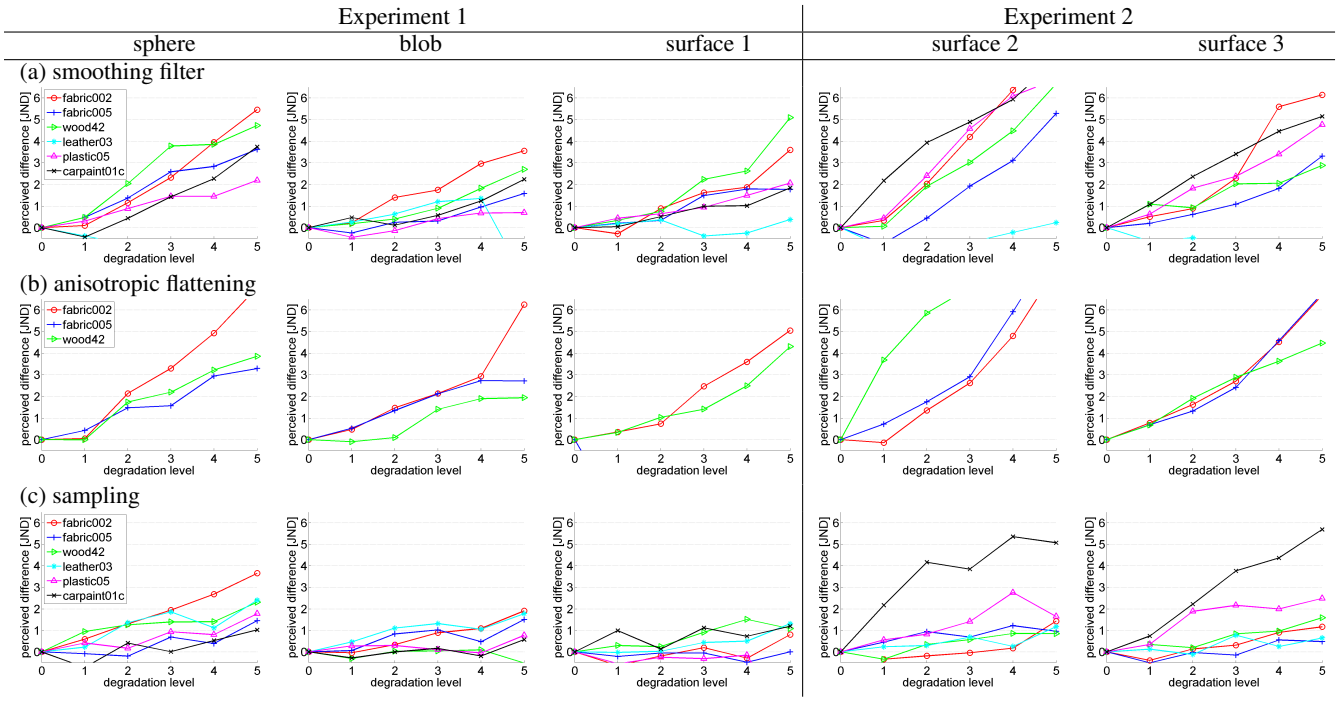


**Figure 10:** *Thurstonian scaling for different BRDF degradation filters (a) smoothing filter, (b) anisotropic flattening, (c) azimuthal resampling.*

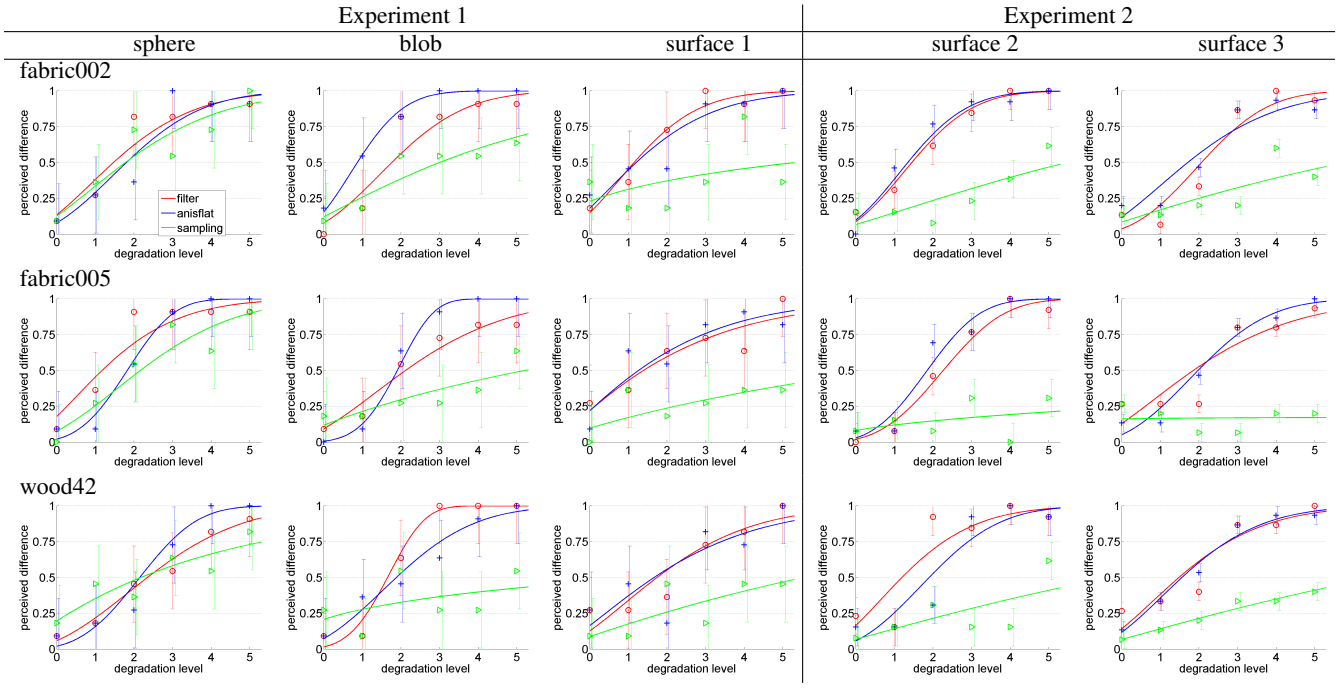


**Figure 11:** *Psychometric functions for different filters and anisotropic materials.*

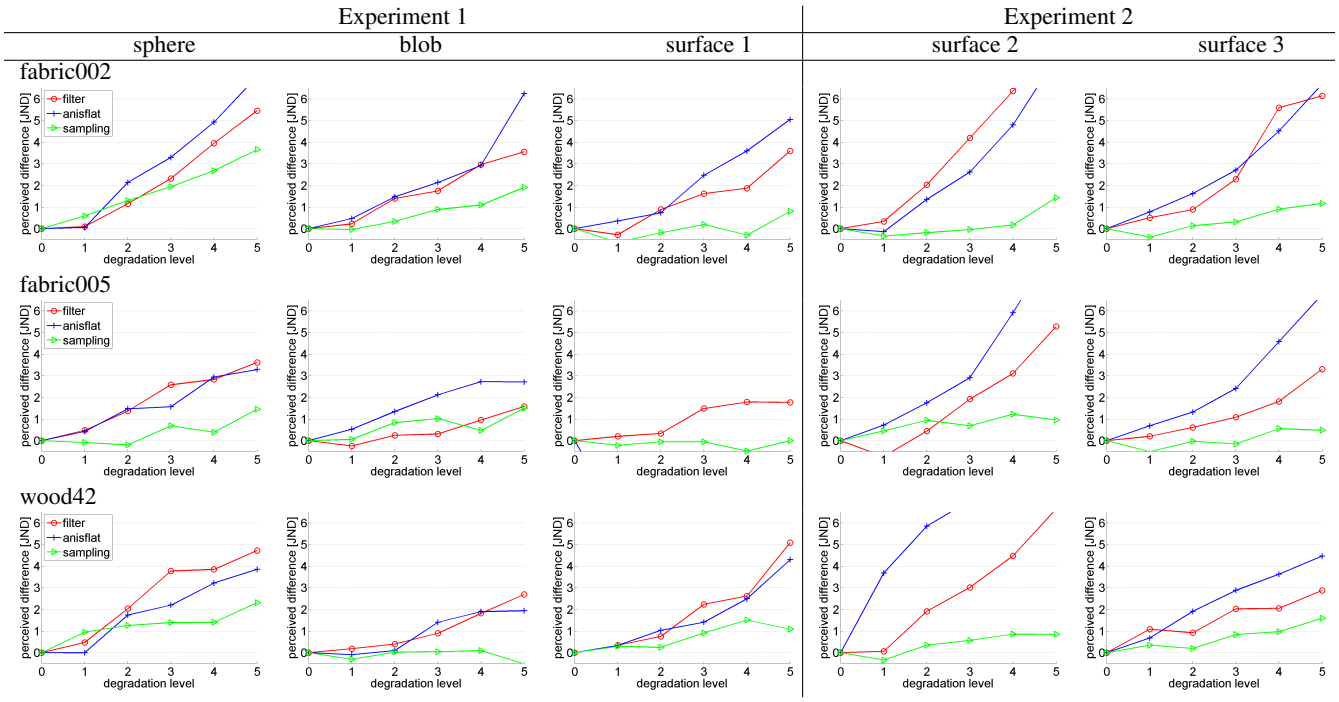


**Figure 12:** *Thurstonian scaling for different filters and anisotropic materials.*

## 5 Results of Computational Image Metrics

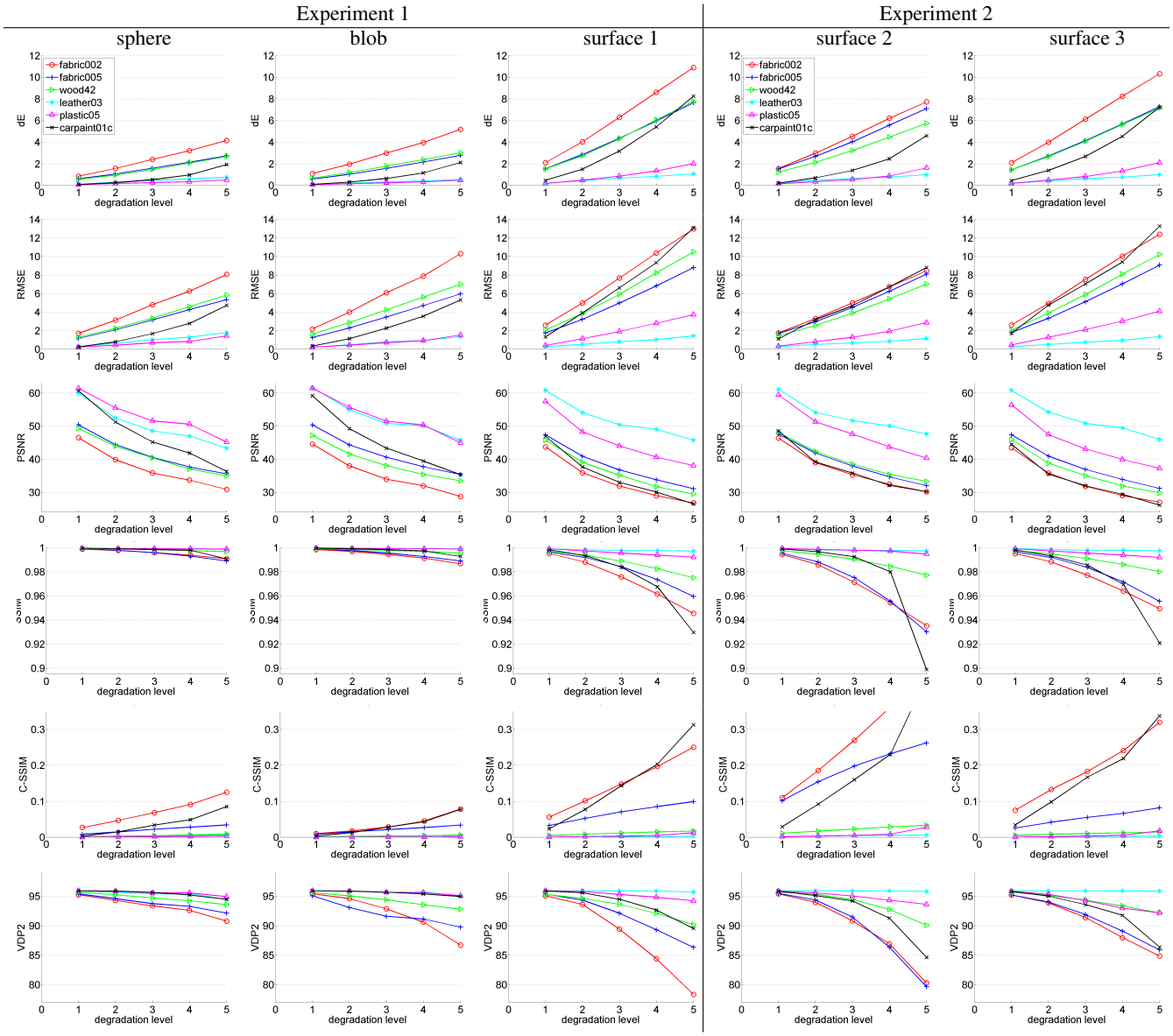


**Figure 13:** *Results of computational image metrics $\Delta E$, RMSE, PSNR [dB], SSIM, C-SSIM, VDP2 for all tested surfaces.*

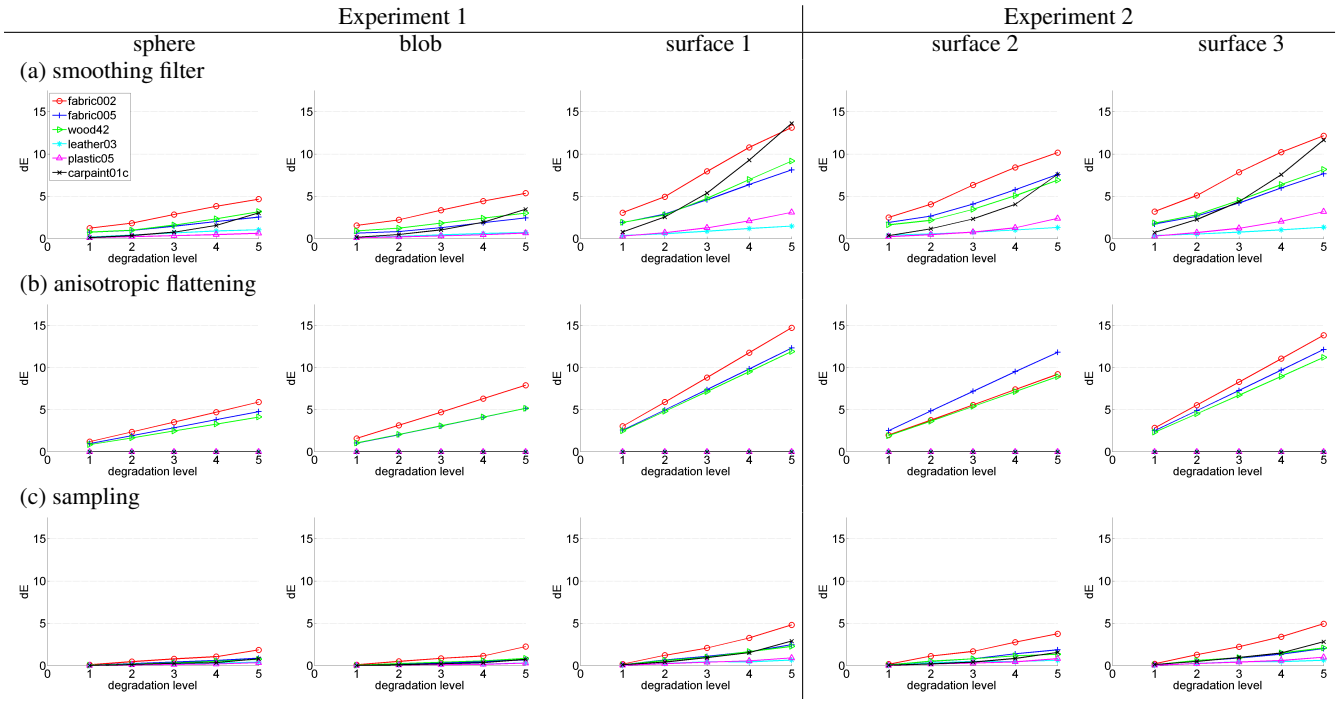


**Figure 14:** *Results of computational image metric $\Delta E$ for individual degradation filters.*

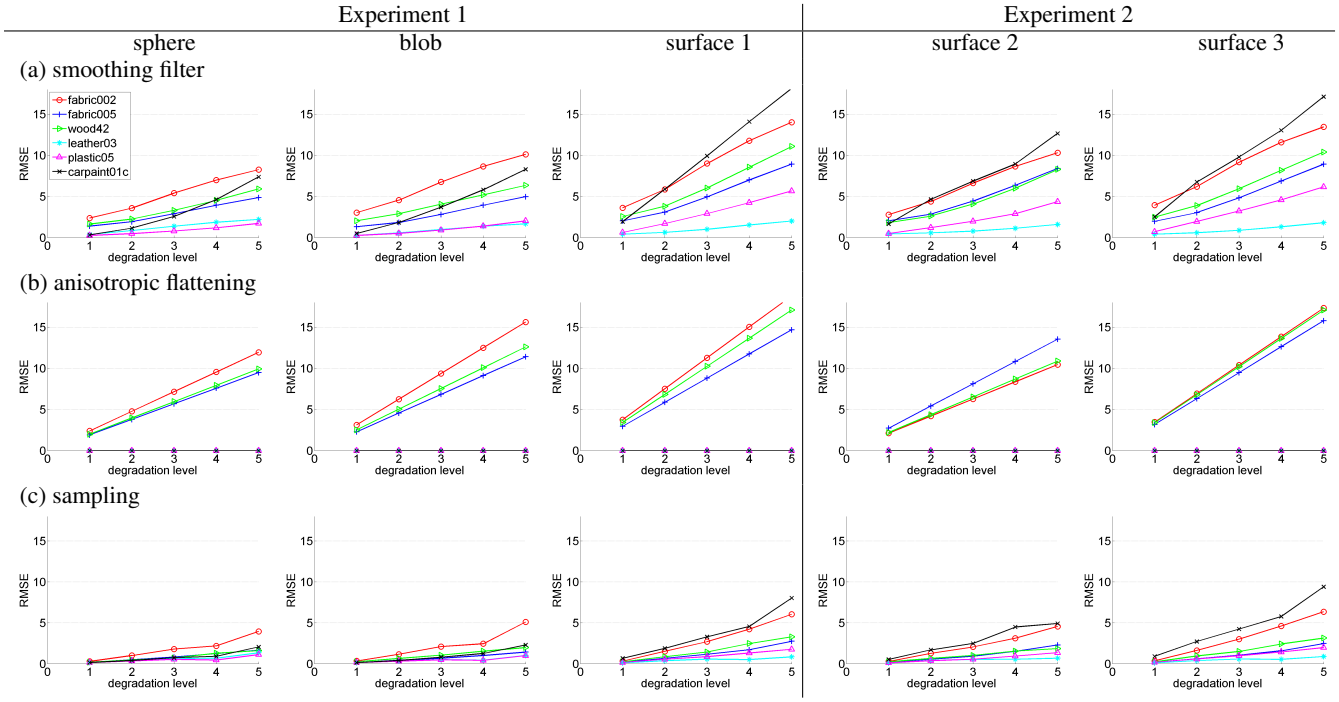


**Figure 15:** *Results of computational image metric RMSE for individual degradation filters.*

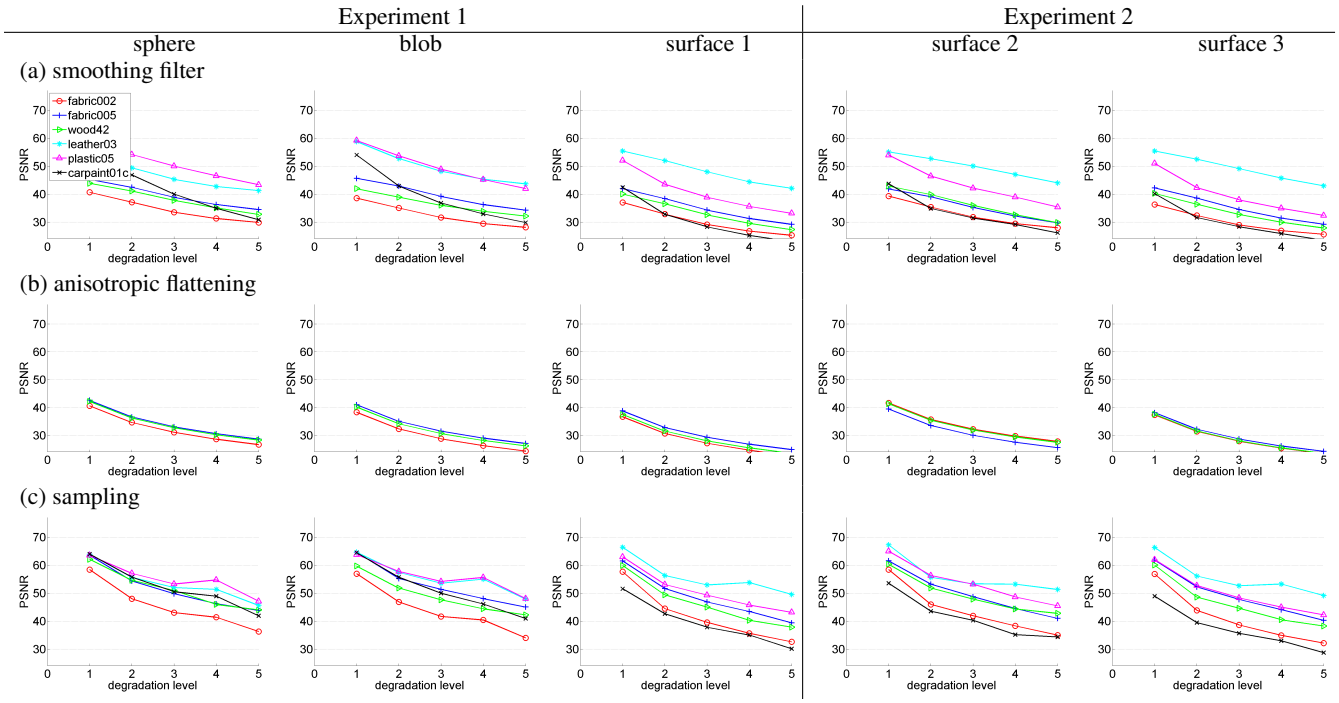


**Figure 16:** *Results of computational image metric PSNR for individual degradation filters.*

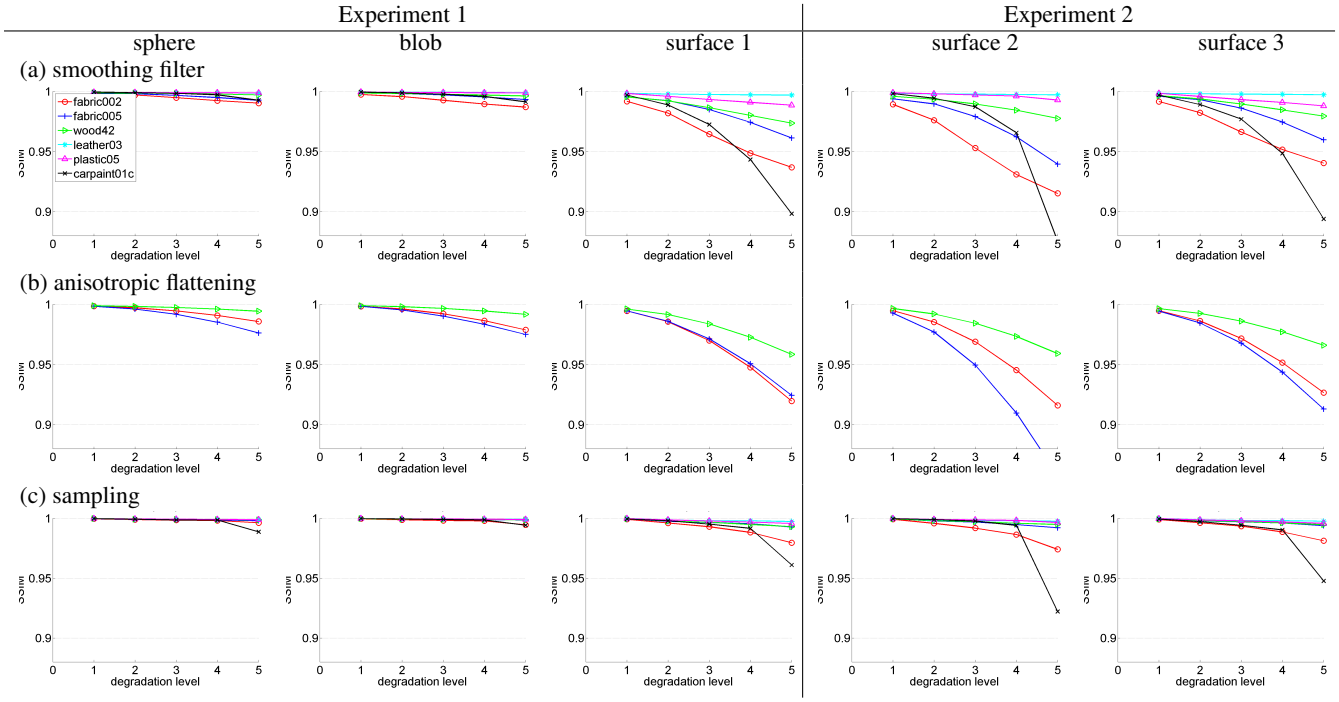


**Figure 17:** *Results of computational image metric SSIM for individual degradation filters.*

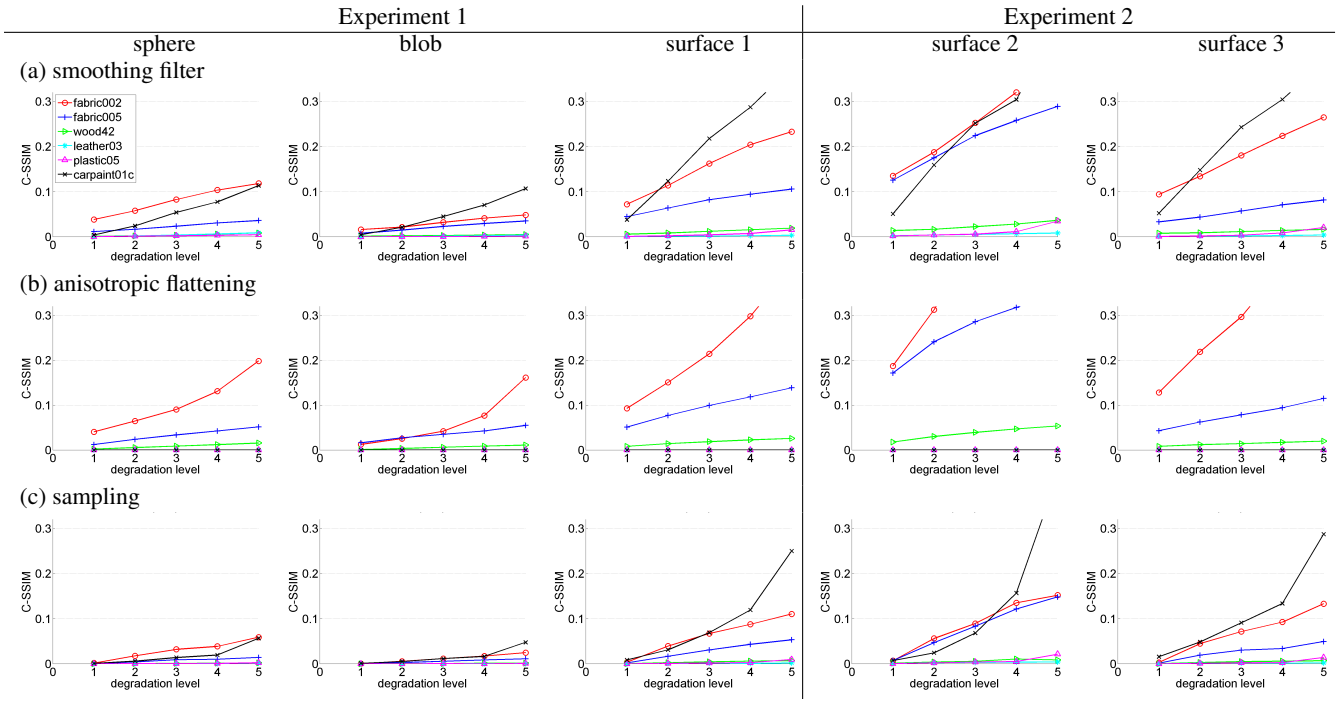


**Figure 18:** *Results of computational image metric C-SSIM for individual degradation filters.*

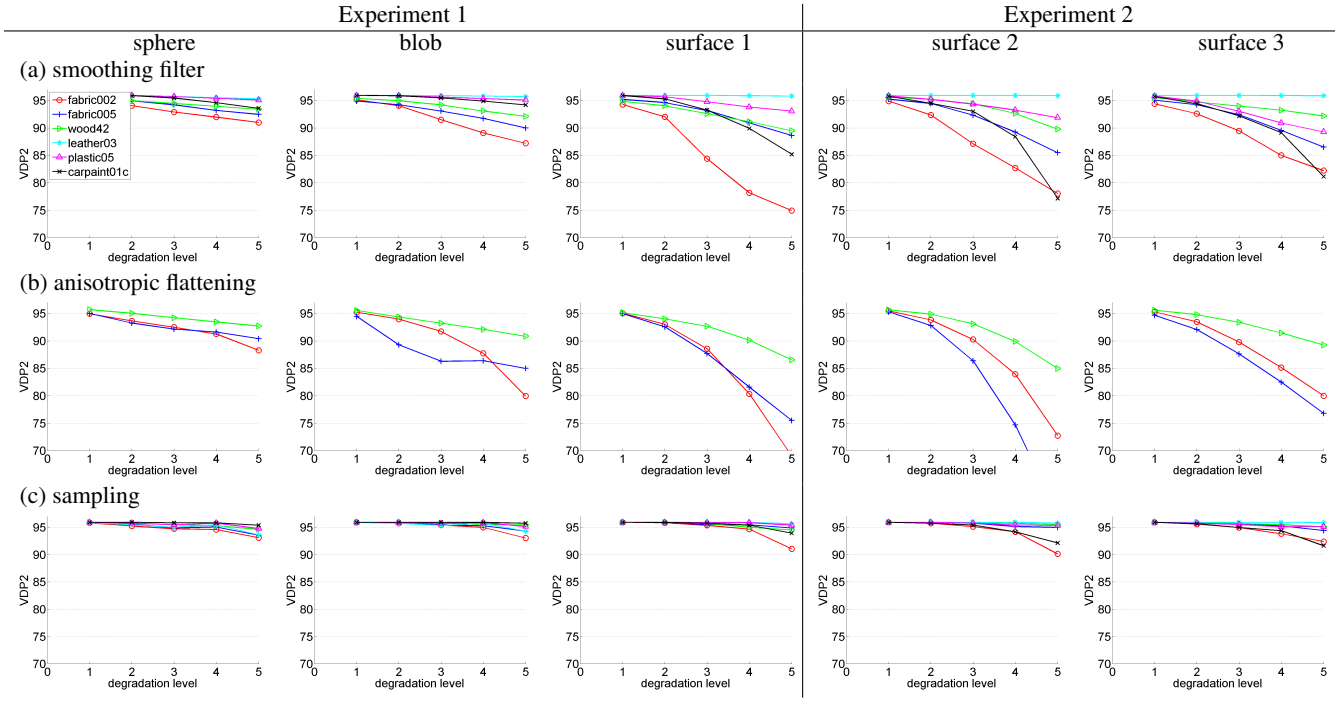


**Figure 19:** *Results of computational image metric VDP2 for individual degradation filters.*

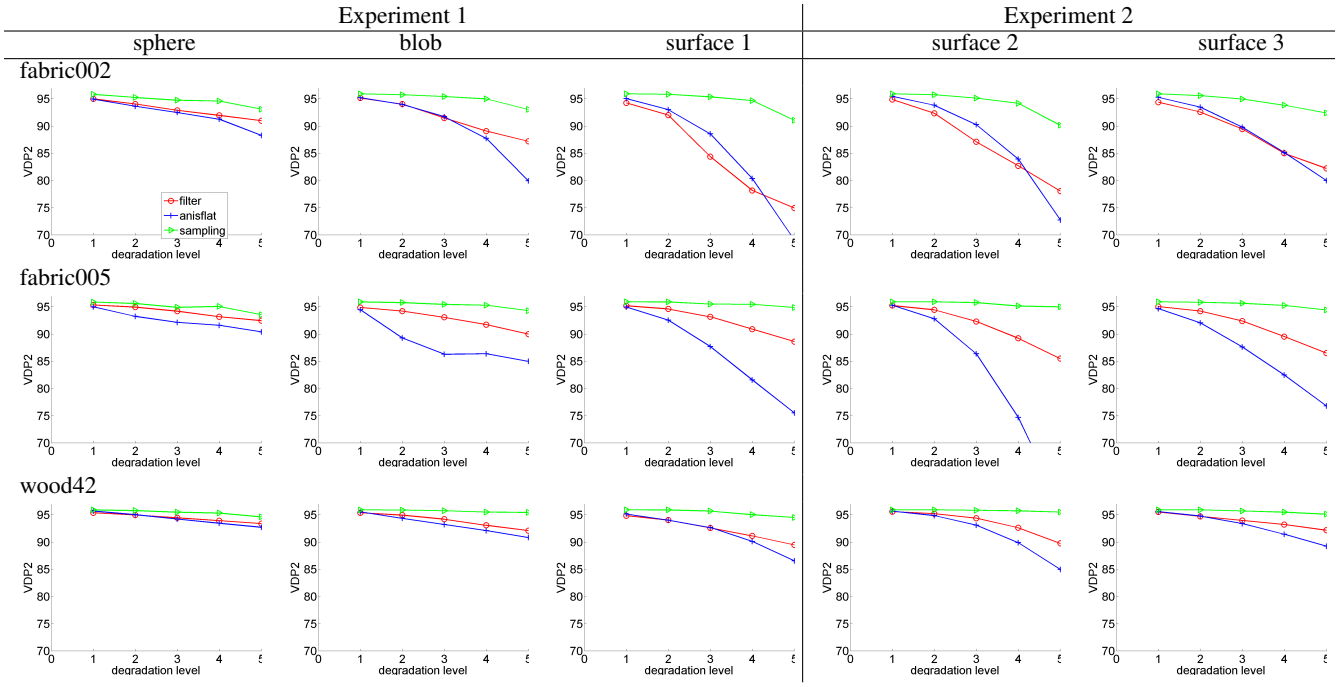


**Figure 20:** *Results of VDP2 for different filters and anisotropic materials.*

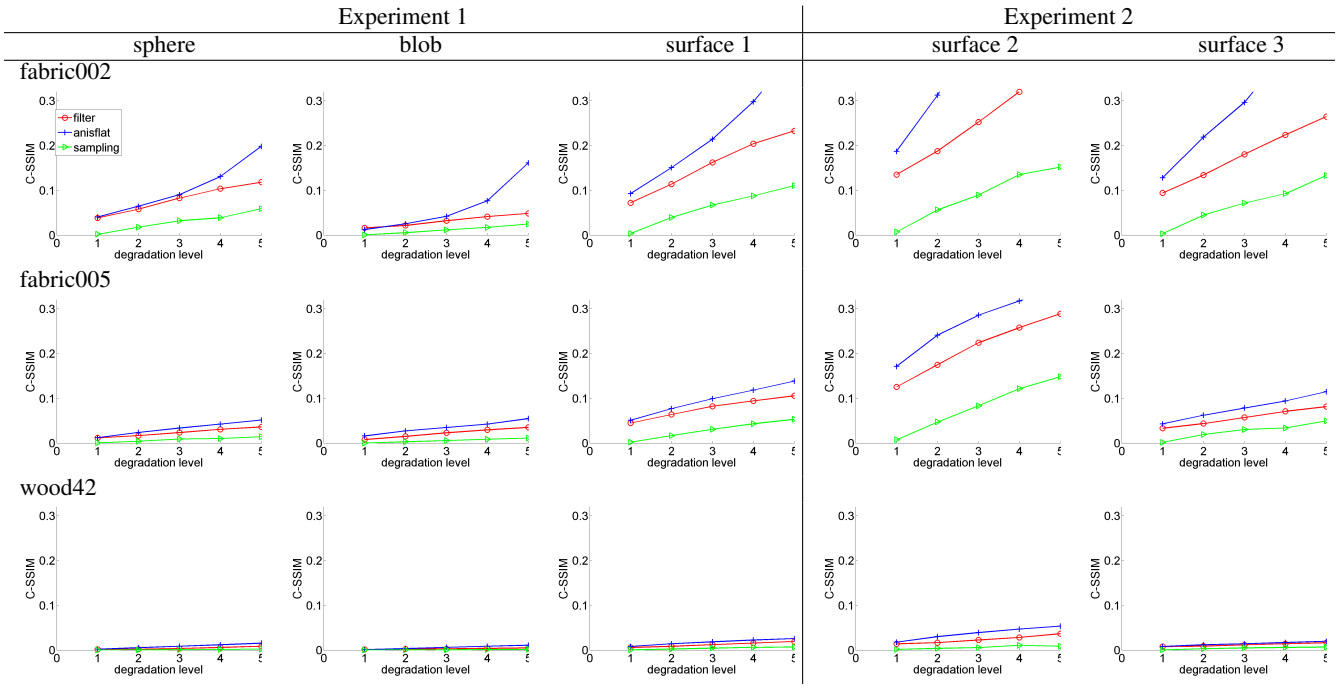


**Figure 21:** *Results of C-SSIM for different filters and anisotropic materials.*

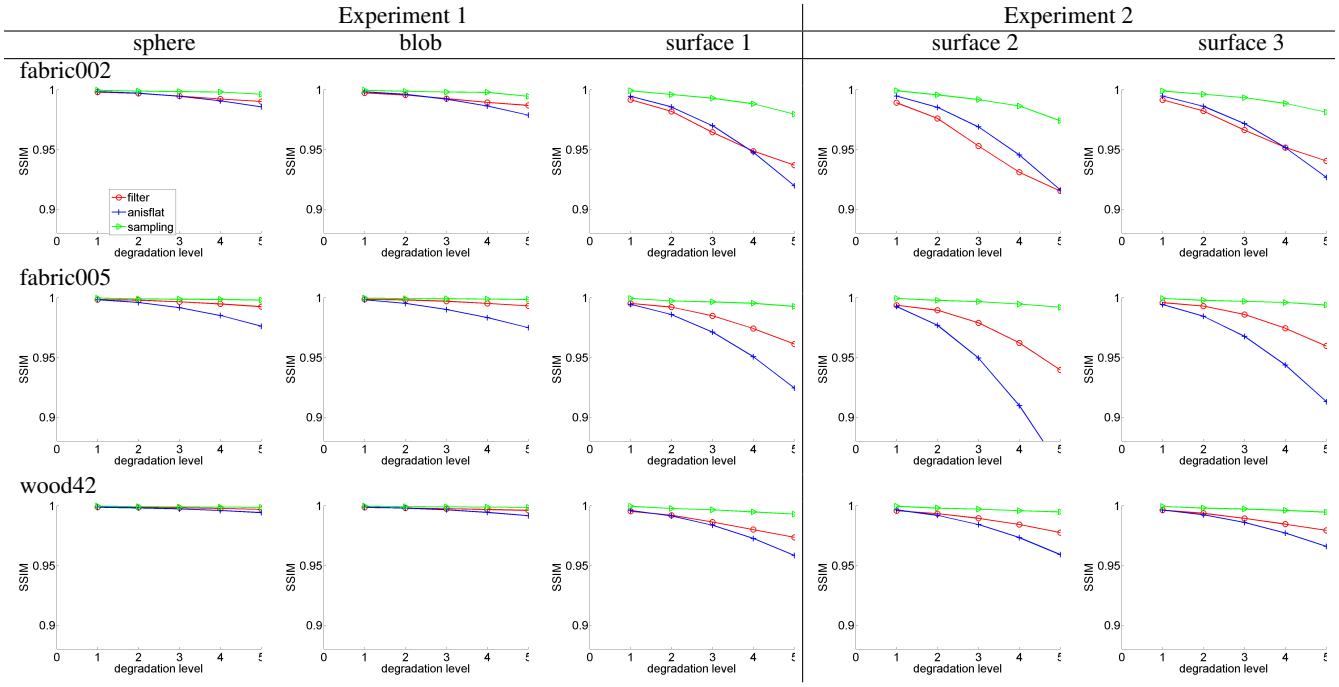


**Figure 22:** *Results of SSIM for different filters and anisotropic materials.*

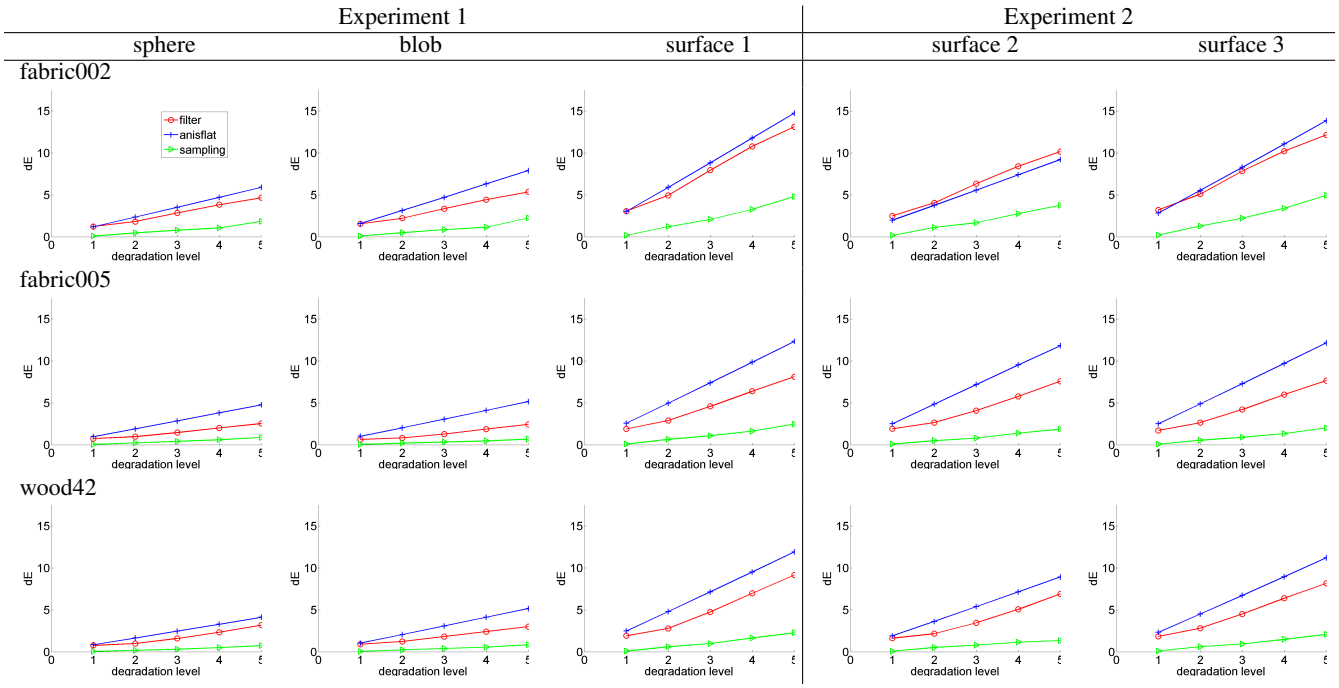


**Figure 23:** *Results of dE for different filters and anisotropic materials.*

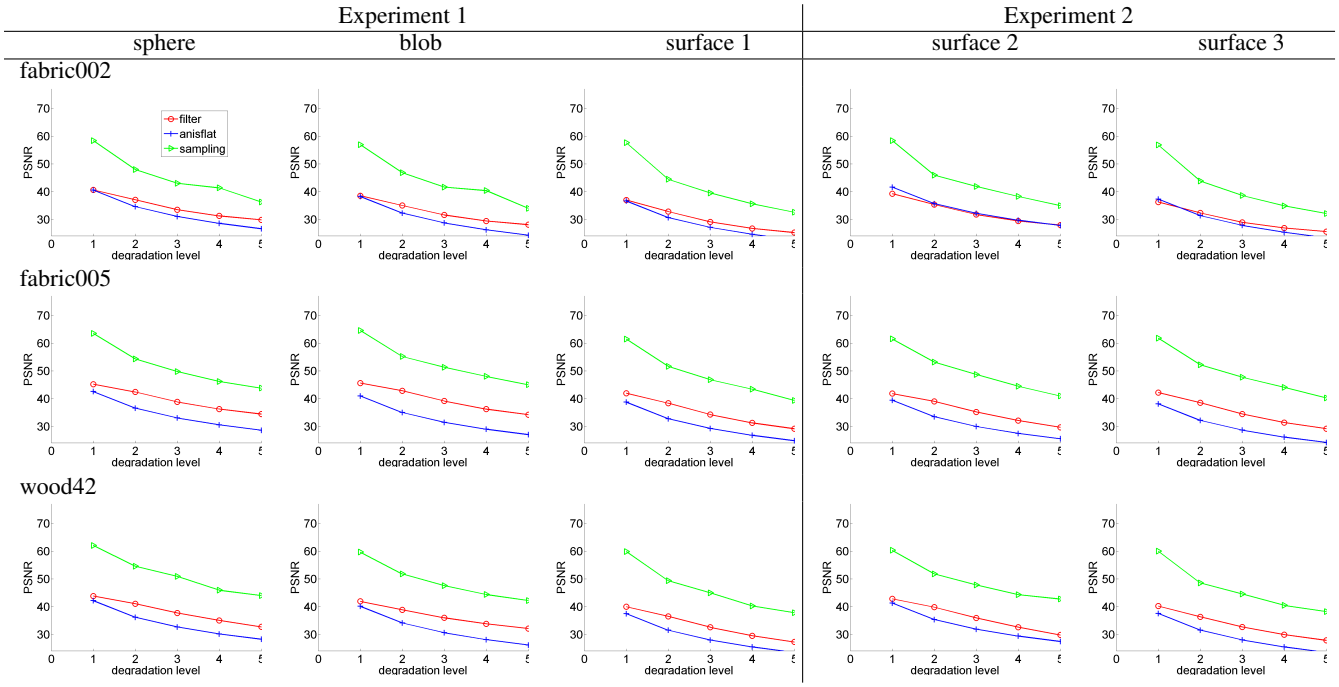


**Figure 24:** *Results of PSNR for different filters and anisotropic materials.*

## 6 Comparing Psychophysics vs. Objective Metrics

Fig. 25, Fig. 26, Fig. 27 compare psychometric and objective metrics for *sphere* and *surface 2* when covered with the anisotropic materials (*fabric002*, *fabric005*, *wood42* respectively). As can be seen the subjects sensitivity for BRDF differences is comparable for both surfaces, while such difference discriminability by objective metrics is much better for *surface 2*.

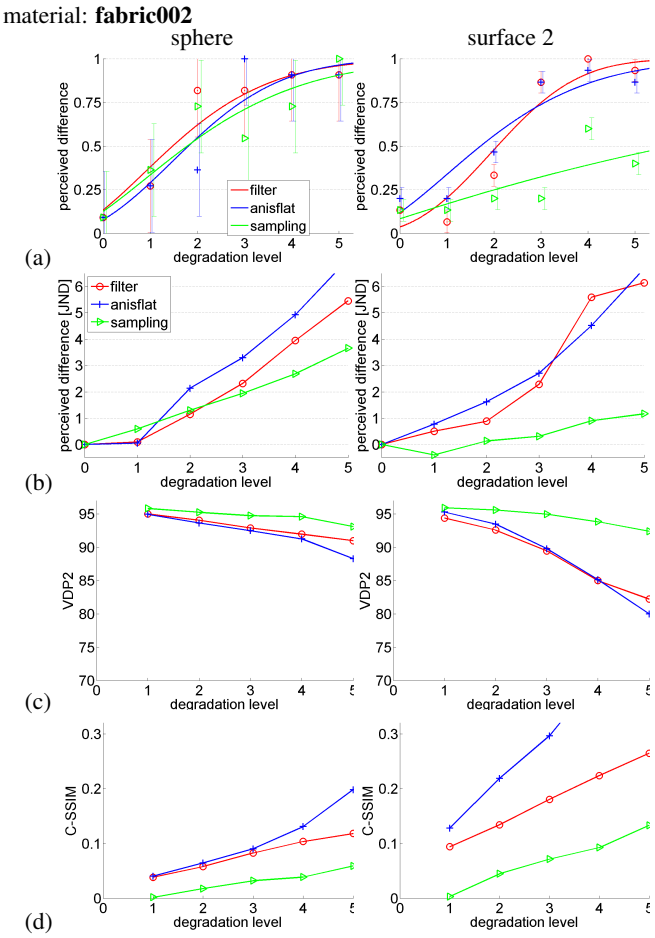


**Figure 25:** *Comparison subjects and computational image metrics performance for individual distortions for material* fabric002*: (a) psychometric functions, (b) Thurstonian scaling, (c) VDP2 (higher is better), (d) C-SSIM (lower is better).*

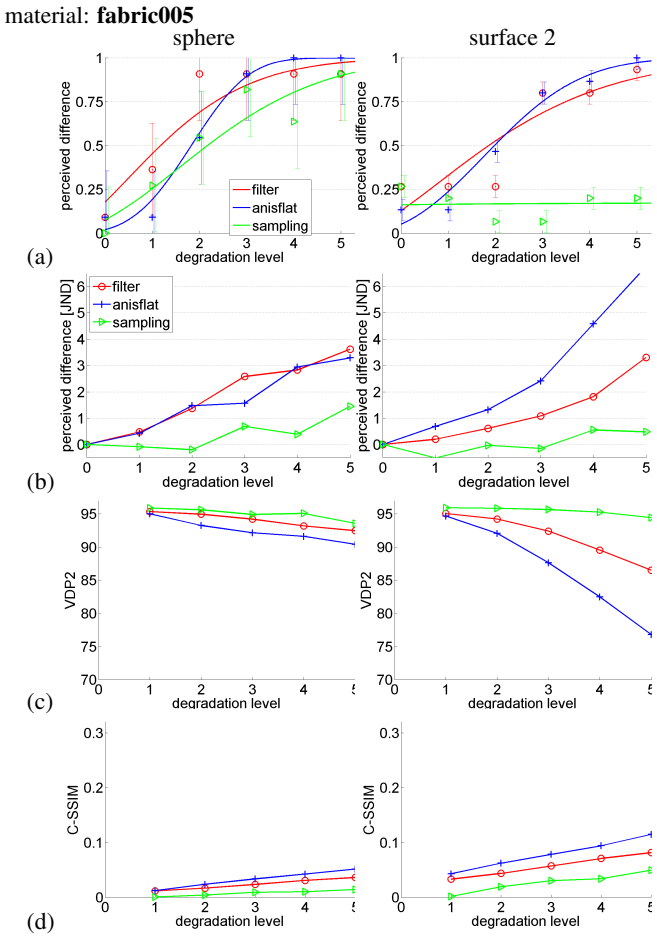


**Figure 26:** *Comparison subjects and computational image metrics performance for individual distortions for material* fabric005*: (a) psychometric functions, (b) Thurstonian scaling, (c) VDP2 (higher better), (d) C-SSIM (lower better).*

material: **wood42**

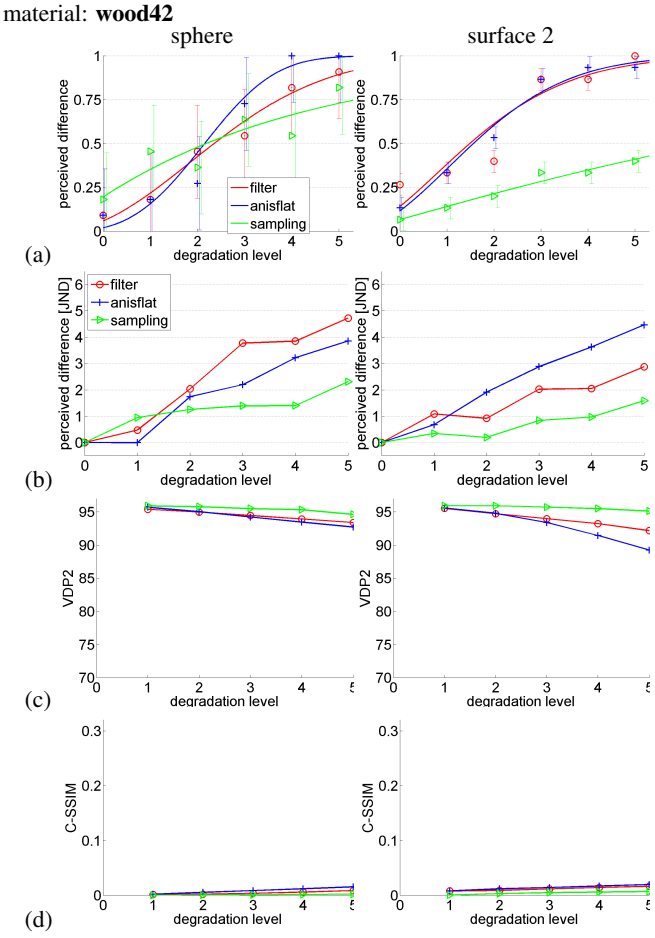


**Figure 27:** *Comparison subjects and computational image metrics performance for individual distortions for material* wood42*: (a) psychometric functions, (b) Thurstonian scaling, (c) VDP2 (higher better), (d) C-SSIM (lower better).*

## 7 Correlations of computational metrics with psychophysical data

We investigated the Pearson and Spearman correlations between subject responses and metric predictions as a function of the surface type. Fig. 28 shows correlation across materials, all degradation filters and also separately for isotropic and anisotropic materials. Fig. 29 shows correlation across materials, for individual degradation filters.

(a) **correlation across materials, all degradation filters**

Pearson

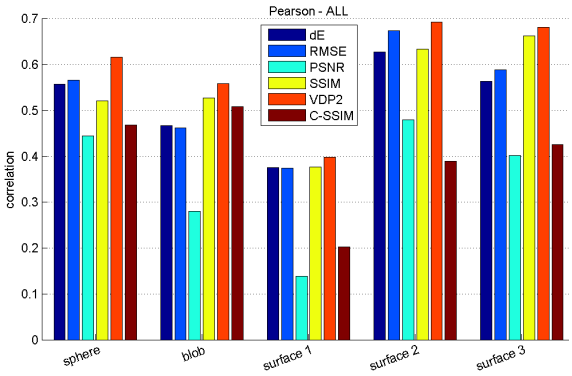


Spearman

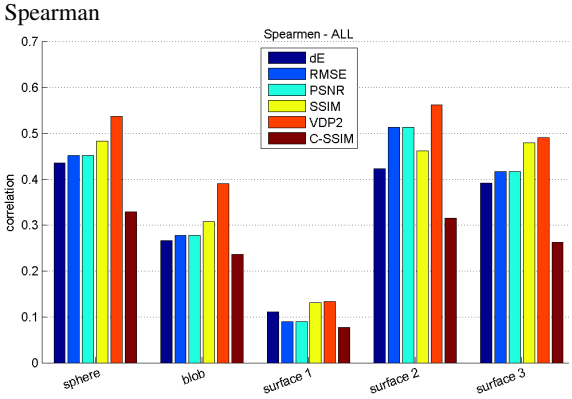


(b) **correlation across anisotropic materials, all degradation filters**

Pearson

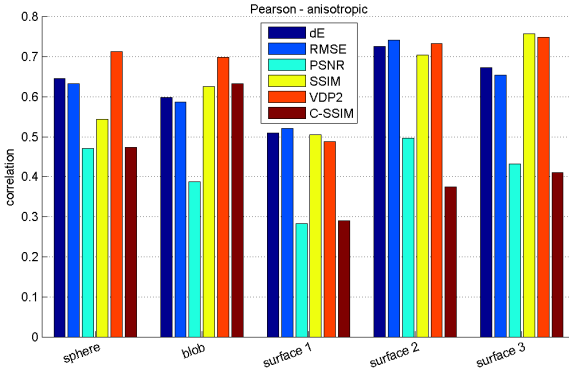


Spearman

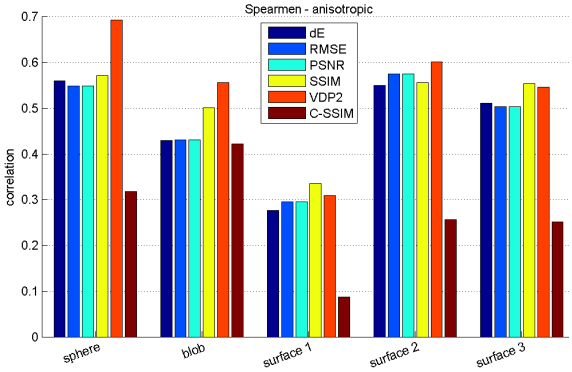


(c) **correlation across isotropic materials, all degradation filters**

Pearson

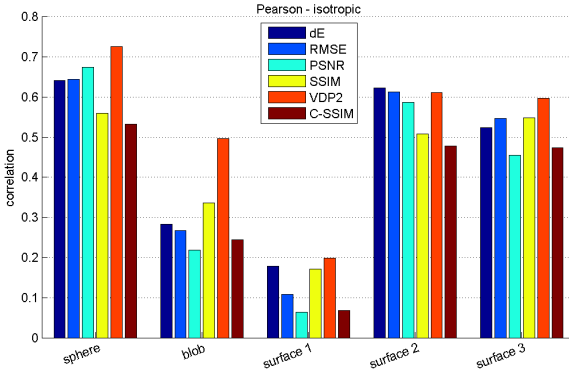


Spearman

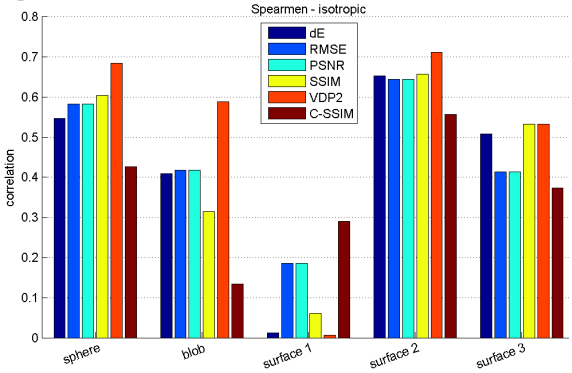


**Figure 28:** *Correlation between Thurstonian scaling data and objective metric. Columns: 1 – Pearson correlation, 2 – Spearman correlation. Correlations are computed across all materials and separately for anisotropic and isotropic ones only.*

(a) **correlation across degradation level 1, all materials**

Pearson

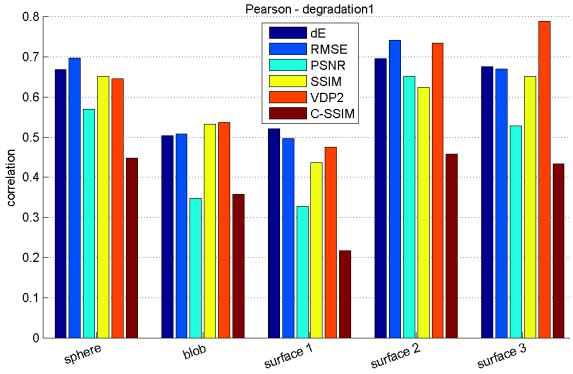


Spearman

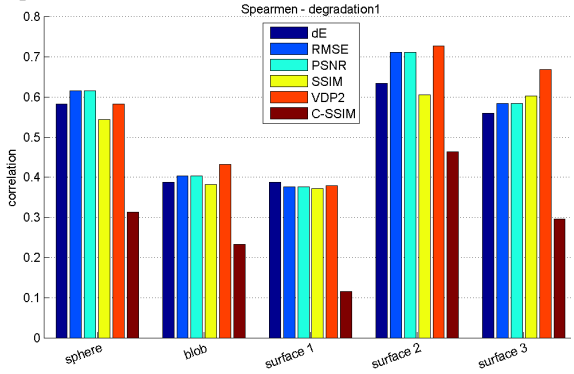


(b) **correlation across degradation level 2, anisotropic materials**

Pearson

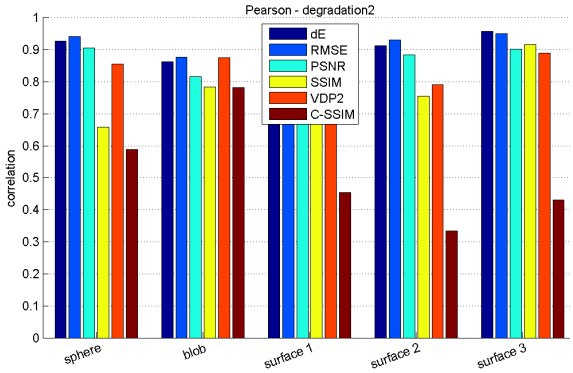


Spearman

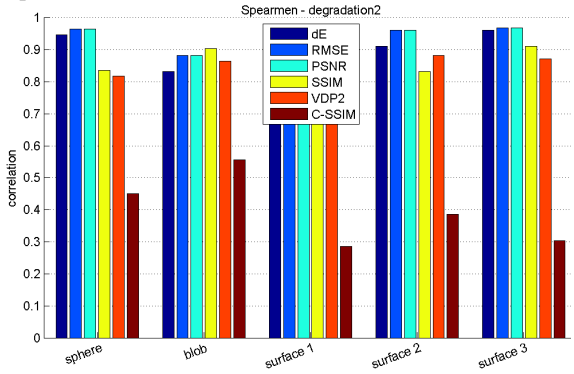


(c) **correlation across degradation level 3, all materials**

Pearson

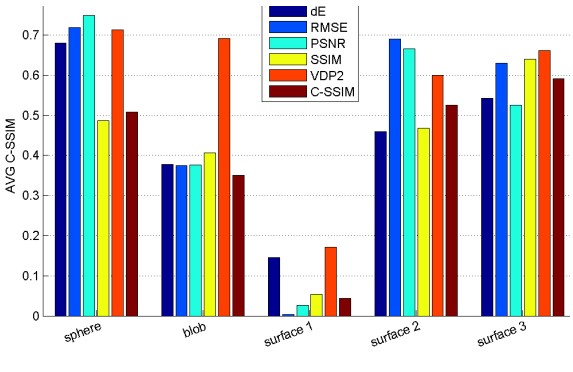


Spearman

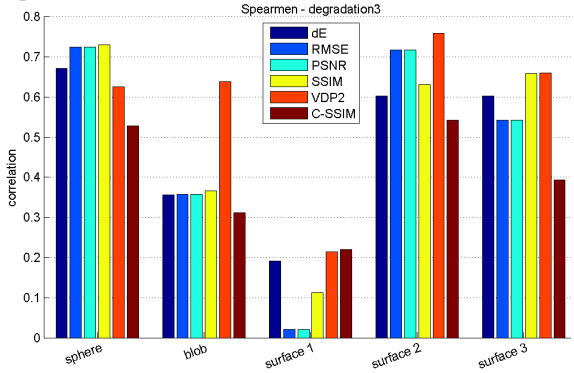


**Figure 29:** *Correlation between Thurstonian scaling data and objective metric. Columns: 1 – Pearson correlation, 2 – Spearman correlation. Correlations are computed for different degradation levels.*

## 8 Application Example: Analytical Models Performance Evaluation

This section illustrates performance of our method when results of analytical BRDF models are compared to the reference BRDF data using computational metrics. Fig. 30 and Fig. 31 show results for Kurt anisotropic model [KSKK10] under environment illumination *grace* and *st.peters*. Fig. 32 and Fig. 33 Kurt anisotropic model [KSKK10] and for anisotropic stencils-based model [FHV15] under point-light illumination.

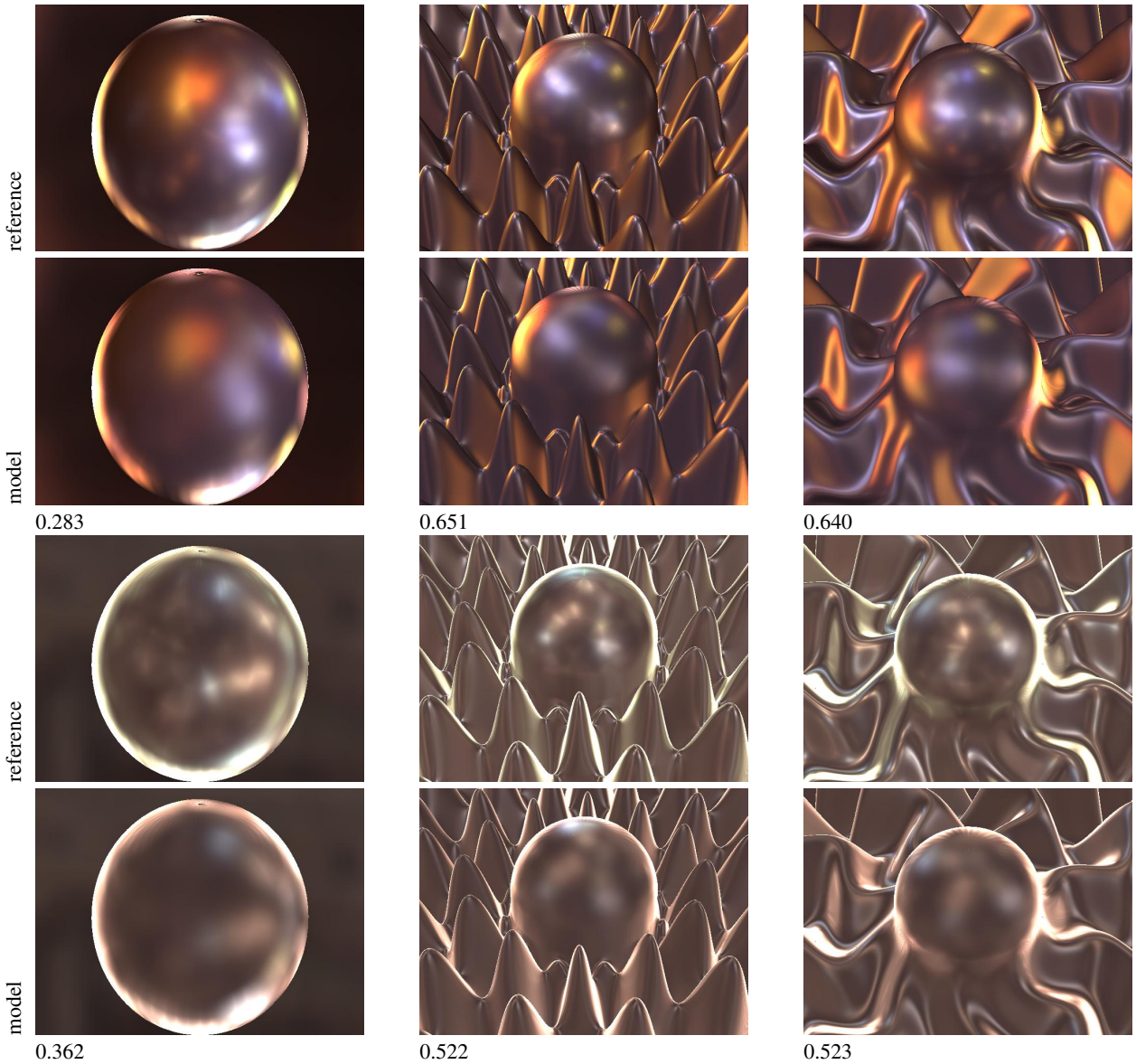


**Figure 30:** *Example of analytic BRDF model performance on different surfaces under environment illuminations* grace *and* st.peters *with corresponding C-SSIM similarity values. Isotropic material* carpaint01.

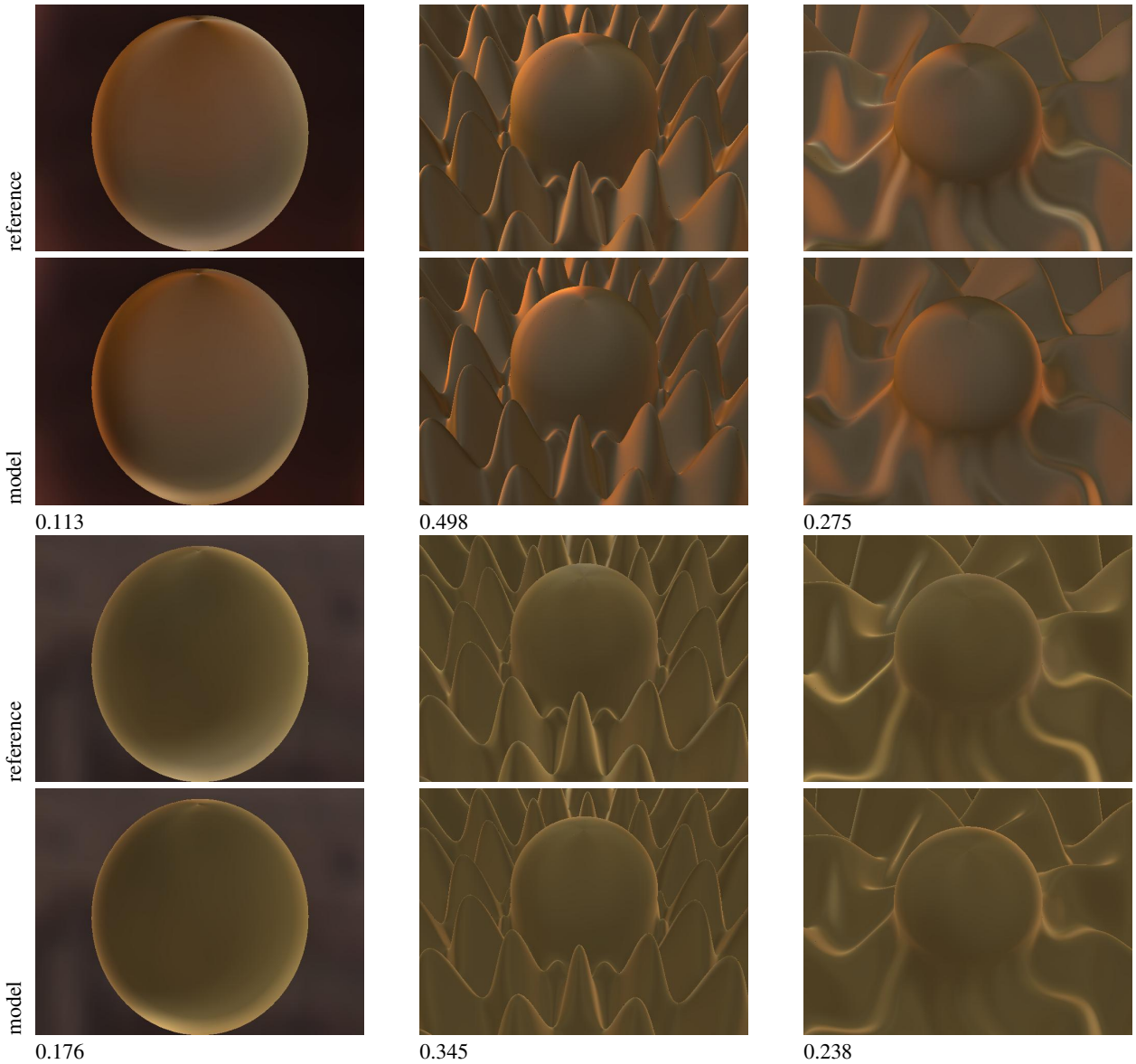


**Figure 31:** *Example of analytic BRDF model performance on different surfaces under environment illuminations* grace *and* st.peters *with corresponding C-SSIM similarity values. Anisotropic material* fabric005.

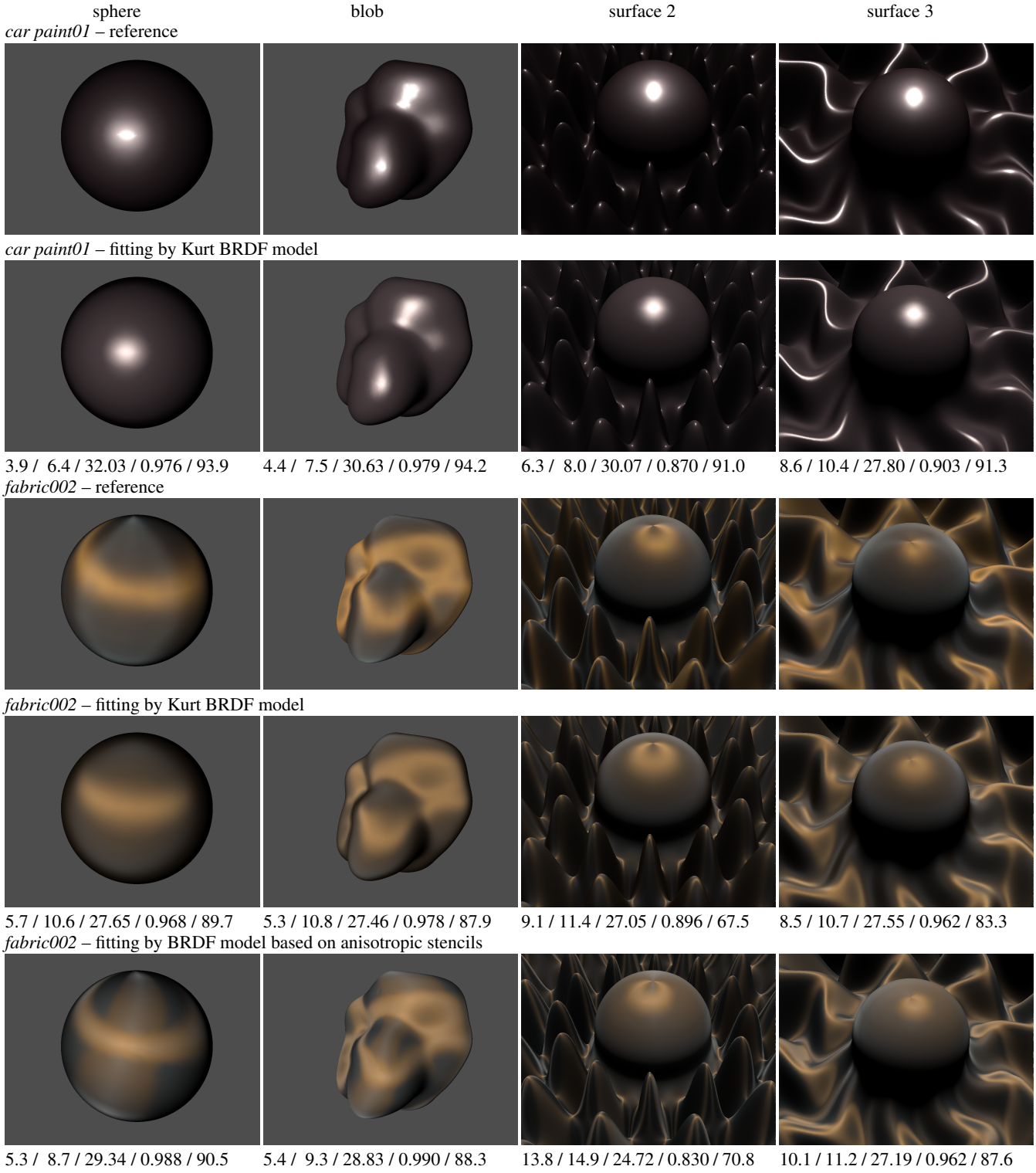


**Figure 32:** *Performance of two BRDF models is evaluated on standard and proposed surfaces: Kurt anisotropic model and anisotropic stencils-based model. Evaluated computational metrics are $\Delta E$, RMSE, PSNR [dB], SSIM, VDP2 respectively.*

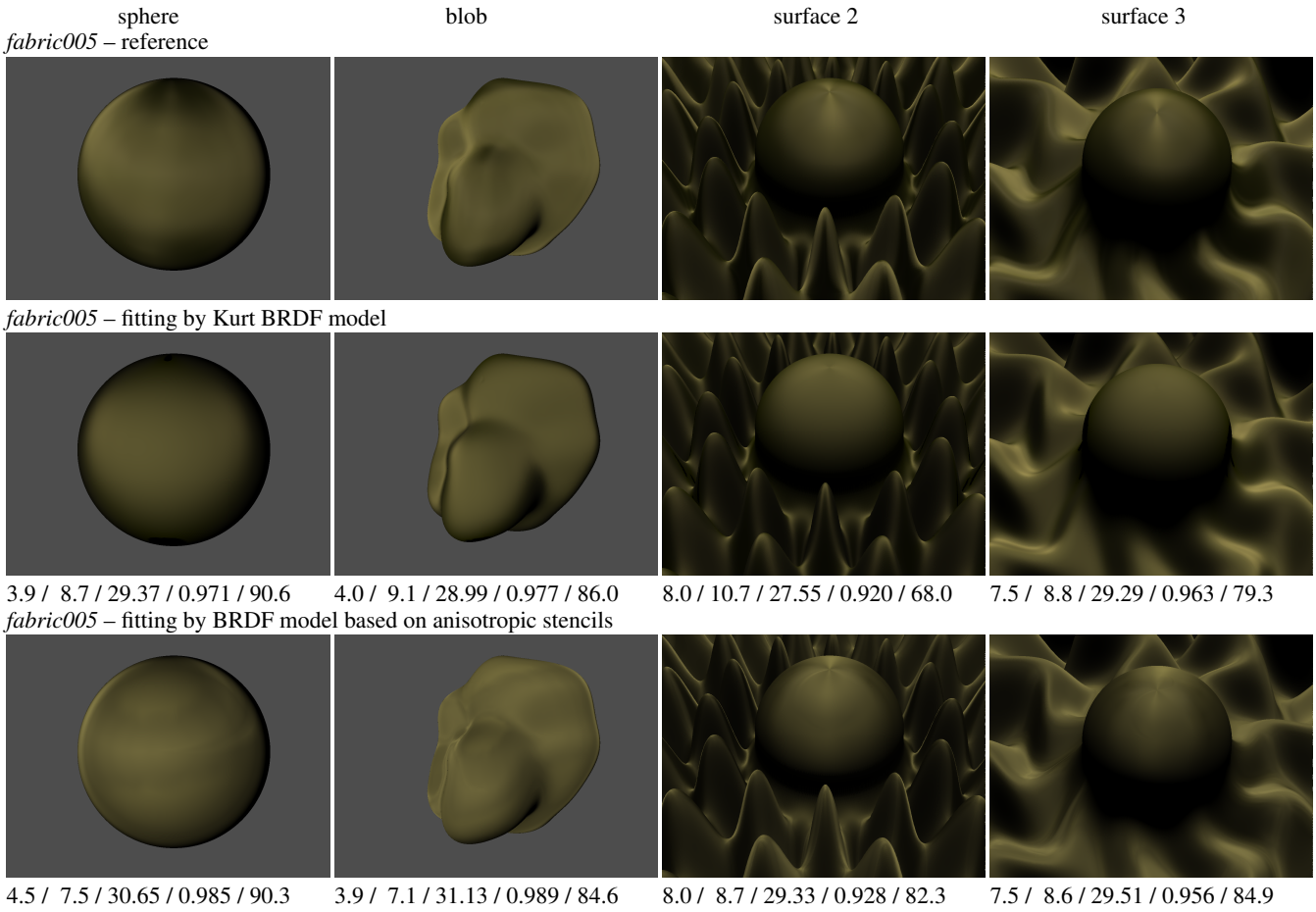


**Figure 33:** *Performance of two BRDF models is evaluated on standard and proposed surfaces: Kurt anisotropic model and anisotropic stencils-based model. Evaluated computational metrics are $\Delta E$, RMSE, PSNR [dB], SSIM, VDP2 respectively.*

## References

FILIP J., HAVLÍČEK M., VÁVRA R.: Adaptive highlights stencils for modeling of multi-axial BRDF anisotropy. *The Visual Computer* (2015), 1–11.

KOUDELKA M., MAGDA S., BELHUMEUR P., KRIEGMAN D.: Acquisition, compression, and synthesis of bidirectional texture functions. In *Texture 2003* (2003), Heriot-Watt University, pp. 47–52.

KURT M., SZIRMAY-KALOS L., KŘIVÁNEK J.: An anisotropic BRDF model for fitting and monte carlo rendering. *SIGGRAPH Comput. Graph. 44* (2010), 3:1–3:15.

LISSNER I., PREISS J., URBAN P., LICHTENAUER M. S., ZOLLIKER P.: Image-difference prediction: From grayscale to color. *IEEE TIP 22*, 2 (2013), 435–446.